



# **MEMS Shock Accelerometers**

## **Signal Modification Attributable to the Electrical Impedance of Their Cables**

Written By

Patrick L. Walter, PCB Piezotronics

Alan Szary, Precision Filters, Inc.

James Woernley, Precision Filters Inc.

**MEMS SHOCK ACCELEROMETER SIGNAL MODIFICATION ATTRIBUTABLE TO THE  
ELECTRICAL IMPEDANCE OF THEIR CABLES**

**FINAL: March 2021**

**Patrick L. Walter  
Measurement Consultant, PCB Piezotronics  
Professor Emeritus, TCU Engineering  
Fort Worth, TX 76129**

**Alan Szary  
VP Engineering & Business Development, Precision Filters, Inc.  
Ithaca, NY 14850**

**James Woernley  
Application Engineer, Precision Filters Inc.  
Ithaca, NY 14850**

**ABSTRACT**

No matter how well designed, an instrumentation system can only correctly condition and record signals from transducers if these signals are transmitted with fidelity via the cable interfacing the transducer to the system. For MEMS (Micro-Electro-Mechanical-Systems) piezoresistive (PR) shock accelerometers, the two main cable concerns are signal modification due to: (1) additive triboelectric noise generated within the cables and/or (2) unknown or unaccounted for electrical impedance characteristics of the cable. Small diameter, lightweight, (e.g. AWG 36) integral, 4-conductor, shielded cables are required for interconnection to the 1.4 grams or less accelerometers. Larger diameter attachment cables would degrade the structural performance of the accelerometer. The effects of triboelectric noise within these small diameter cables has been documented and solutions provided.<sup>4</sup> The subject of this research is the influence of the electrical impedance of the cable on the gamut of MEMS accelerometers designed to operate in severe shock environments. This influence is primarily a function of the combined cable/MEMS element high frequency RC time constant. Challenges exist in determining this time constant, and a method is proposed for accurately predicting system frequency limitations posed by *individual* cable and sensor characteristics. Electrical bench testing has verified the accuracy of these predictions. A hardware solution, *AC Shunt Calibration*, is provided to determine in-situ instrumentation system frequency constraints accurately and efficiently prior to test initiation.<sup>6</sup> Last, mechanical shock testing was performed and was shown to correlate with results of the electrical bench testing.

## INTRODUCTION

In 2019, PCB Piezotronics executed an agreement with Meggitt PLC (MGGT.L) to purchase the assets of its Endevco sensor business. Not surprisingly, the sensor product lines of Endevco, established in 1947, and PCB, established in 1967, overlapped in many areas. In the aerospace and defense (A&D) sector, the strong suit of both companies lay in manufacturing accelerometers to measure severe mechanical shock. Examples of these shocks are encountered in structures exposed to impact and explosive loading. PCB had previously developed a line of mechanically isolated piezoelectric accelerometers with incorporated electronics (ICP®) and low-pass filters (e.g., model 350DO2). These had been verified to yield excellent shock reproduction at frequencies up to 10 KHz at acceleration levels up to and exceeding 10's of thousands of Gs.<sup>1</sup> The significant overlap in products was between the two companies' MEMS (PR) based accelerometers. Micro-Electro-Mechanical Systems, or MEMS, represent a technology that evolved from the semiconductor device fabrication market. It can be defined as miniaturized mechanical and electro-mechanical elements (i.e., devices and structures) that are made using the techniques of microfabrication. The critical dimensions of MEMS devices can vary from well below one micron, on the lower end of the dimensional spectrum, up to several millimeters. The competitive MEMS-based accelerometer models for severe shock, with ranges of 20,000 G or above, are listed in the first two filled columns of TABLE 1 below.

MEMS (PR) ACCELEROMETERS FOR SEVERE SHOCK							
MODEL	RANGES (KG)	MINIMUM Rout OHMS	MAXIMUM Rout OHMS	SUPPLY VOLTS V	F.S. OUT (NOMINAL) (mV)	RESONANT FREQUENCY (KHZ)	USEABLE FREQUENCY (KHZ)
ENDEVCO 7270A	20	350	950	12 MAX	200 typical @ 10V	350	50
	60	350	950	12 MAX	200 typical @ 10V	700	100
	200	350	950	12 MAX	200 typical @ 10V	1,200	150
				DAMPING < 0.007 CRITICAL NO MECHANICAL STOPS			
ENDEVCO 7280A	20	4000	9000	12 MAX	300 typical @ 10V	100	10
	60	4000	9000	12 MAX	300 typical @ 10V	130	13
					DAMPING < 0.04 CRITICAL MECHANICAL STOPS		
PCB 3991	20	4000	8000	15 MAX	200 typical @ 10V	>60	10
	60	4000	8000	15 MAX	200 typical @ 10V	> 120	20 (1dB)
					DAMPING < 0.04 CRITICAL MECHANICAL STOPS		

**TABLE 1: Competitive Endevco and PCB MEMS (PR) Shock Accelerometer Models (current 2019)**

A first review of the individual data sheets for the three accelerometer models pictured in TABLE 1 indicates few differences between them. They all have the same geometric form factors, weigh approximately 1.4 grams, mount with 2 each 4-40 screws, require torques of 8 +/- 2 inch-pounds, have integral 4-wire stranded 36 AWG insulated conductors with an outer cable shield and jacket, and have nominally the same sensitivity with comparable supply voltages. A detailed test series performed at National Test Systems (NTS) compared representative models of MEMS based accelerometers under conditions of severe shock.<sup>2</sup> Based on shock response spectrum (SRS) analysis of their measured signals, they performed comparably.

TABLE 1 presents a subset of specifications allowing a more detailed comparison. Note the output resistances of the accelerometers vary in the extreme by a ratio of 26:1 (9,000 ohms to 350 ohms) across the different models. In addition, the useable frequency capabilities specified across the 3 models/ranges vary by a factor of 15:1 (150 KHz to 10 KHz). Last, again note the cable is an integral feature of the accelerometer. The cable can be provided in any length that the customer requests. To the extent that the cable can be modeled in terms of its parallel line capacitance and series resistance, it has the potential to modify (i.e. filter) the accelerometers' output signal. To a first-order approximation, the "cutoff" or -3dB limitation induced by this filtering is controlled by the accelerometers' output resistance (R) and cable capacitance (C). The reciprocal of this product (RC = seconds) is the filter's -3 dB frequency ( $\omega_c$ ) in radians/second. RC is defined here as the **high frequency** time constant  $\tau$ . If  $\omega_c$  is divided by 2 pi ( $2\pi$ ) the value of the filter cutoff frequency ( $f_c$ ) in Hz is  $[0.159/(RC)]$ . The complete description of this 1<sup>st</sup> order filter, normalized to its "cutoff" frequency, is presented in Figure 1. Note that the filter can attenuate the high frequencies encountered in severe shock while also phase shifting them (e.g., 45 degrees at  $\omega/\omega_c = 1$ ). Both plots are solely a function of the RC product; that is, the **high frequency** time constant  $\tau$  controls the frequency content that passes through the cable. Recall that R varies between and within accelerometer models and C varies with cable length. The fact that R varies widely within a model is primarily associated with differences between the silicon wafers and their contained dies resulting from the microfabrication process.

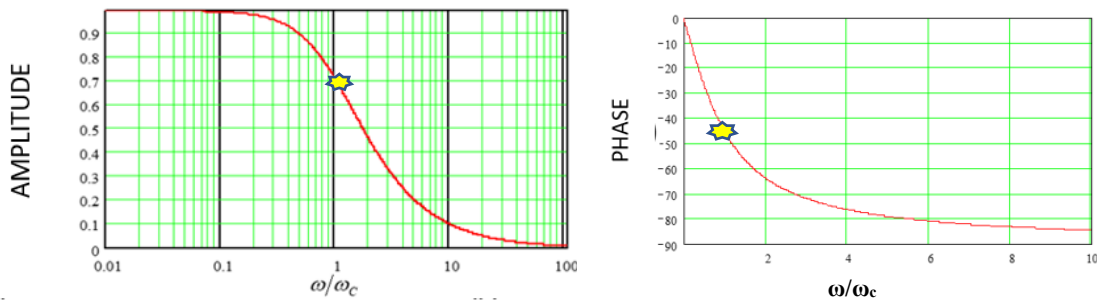


**Figure 1: Amplitude (Left) and Phase (Right - in degrees) Plots vs their Normalized Frequency Response for a 1<sup>st</sup> Order Low-pass Filter (RC =  $\tau$ )**

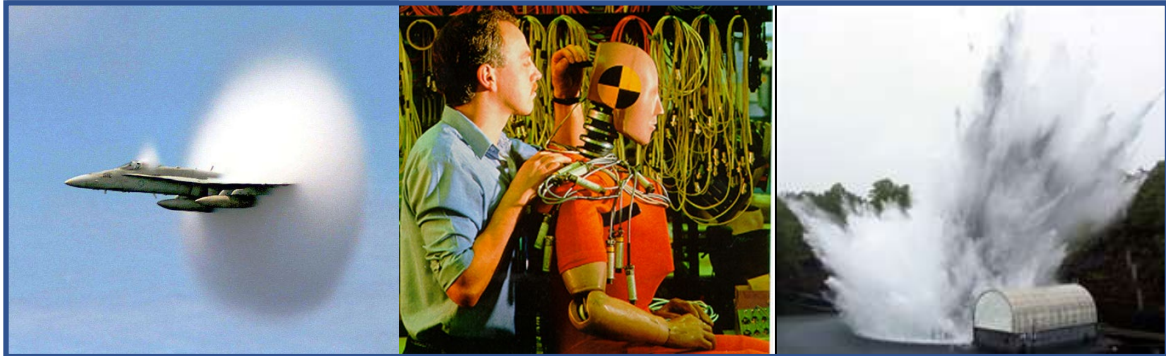
Predictive models will subsequently be developed and validated in this work to enable specification of the high frequency limitation in a measured shock pulse due to the RC product  $\tau$  (time constant) of the accelerometer/cable combination.

### SEVERE SHOCK

Severe shock, as defined here, possesses at least two of the following three (3) attributes: a broad frequency spectrum, high acceleration levels, and high energy. Examples that satisfy these criteria follow:



**Penetrating a Concrete Target**



**Sonic Boom**

**Crash Testing**

**Navy Barge Shock**

**Figure 2. Examples of Severe Shock**

In the environments of Figure 2, critical components must often survive and remain functional during and even after the event. It is imperative to measure the shock these components encounter during the event. For safety considerations, this often involves running long cables to a “hardened” instrumentation room (Fig. 3A). Alternately, a hardened and versatile “junction box” (Fig. 3B) may be a permanent part of the test facility. In this case, sensor cables are transitioned at the “box” to already existing facility cables, which are extended far enough to eliminate the need for a hardened instrumentation room. Thus, whether due to damage during a test or the requirement for additional length, accelerometer cables often are spliced to various other cable extensions.

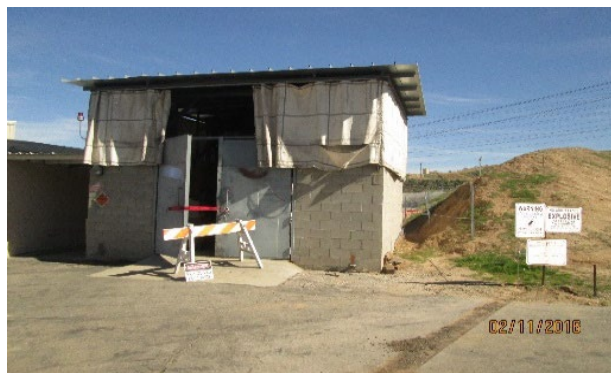


**Figure 3A. Hardened Instrumentation Room**

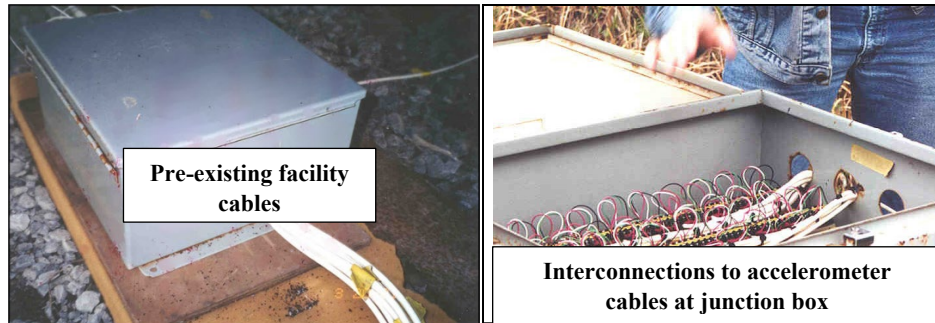


**Figure 3B. Hardened Junction Box Showing Cable Transitions**

**Figure 3. Cable Runs Become Lengthy in Severe Shock Environments**

The necessary steps to design an instrumentation system to measure and record these shocks are defined in reference 3. Step 5 references the cable.

“5. *The sensor’s cable must be carefully selected.* The cable has resistance, capacitance, and inductance. If its influences are not understood and accounted for, it can attenuate signals and induce unwanted filtering. It can also be a signal source attributable to cable induced triboelectric effects. In addition, if not properly shielded, it can also couple undesired electromagnetic and electrostatic fields into the signal. Wear, bend radius, and thermal capabilities are but a few additional cable selection considerations.”

Reference 4 discusses how the cable capacitance and resistance can limit the signal fidelity of MEMS PR sensors. Unlike ICP® shock measurements, with low output impedance where long cable runs are typically co-axial and cable capacitance is easily measured, the cables supporting MEMS sensors are more complex. As noted previously, MEMS sensors require as a minimum 4 conductors, each in its own insulated jacket, an outer conductive shield, and a final insulated jacket over the assembly. In addition, operating into a differential amplifier (typical), the electrical grounding of the shield must be properly managed.

**\*PROBLEM MODELING**

To investigate how the time constant of the accelerometer/cable combination can constrain the upper frequency limitation of the measurement, a basis is needed for comparison (i.e., a recognized standard). Since many of these severe shocks are associated with military applications, an existing military standard (MIL-STD-810H (METHODS 516.8 and 517.3 ANNEX A)) will be referenced for instrumentation requirements over the measurement passband of interest. *For single shocks, MIL-STD-810H requires a pass-band flatness of +/- 1 dB and phase linearity to within +/- 5 degrees across the frequency bandwidth of interest (0 -  $f_{max}$ ). If  $f_{max}$  is not specified, a default value of 10 KHz is recommended.* Keep in mind, other government agencies (NASA, DOE, ...), organizations, companies, and individuals are free to generate their own requirements.

Figure 4 (left) shows the Bode plots (Amplitude and Phase Vs. Frequency) for an idealized shock accelerometer model. The model’s initial 180 degree phase offset simply reflects that fact that an accelerometer’s mass motion relative to its base acceleration occurs in an opposing direction. As expected, the model predicts this. The phase shift at the accelerometer’s natural frequency is always + 90 degrees [-90 - (-180)] = +90. The Bode plots for an idealized RC low-pass filter cable model that it interfaces with are shown in Figure 4 (right). The abscissa for each plot shown (4 total) is normalized to the -3dB frequency of the low-pass cable model. Note that the natural frequency ( $f_n$ ) of the accelerometer in these plots is five times the cable -3dB frequency. For example, if this was to represent a PCB 3991A-20K model/range, with an  $f_n$  of 70 KHz,  $f_{-3dB}$  would be 14 KHz ( $f_n/5$ ).

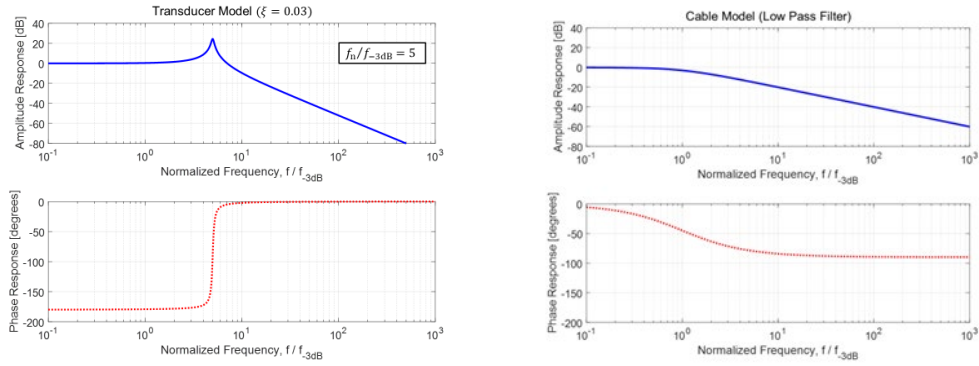


**Figure 4. Idealized Accelerometer Model Left and Idealized Low-pass Cable Model Right**

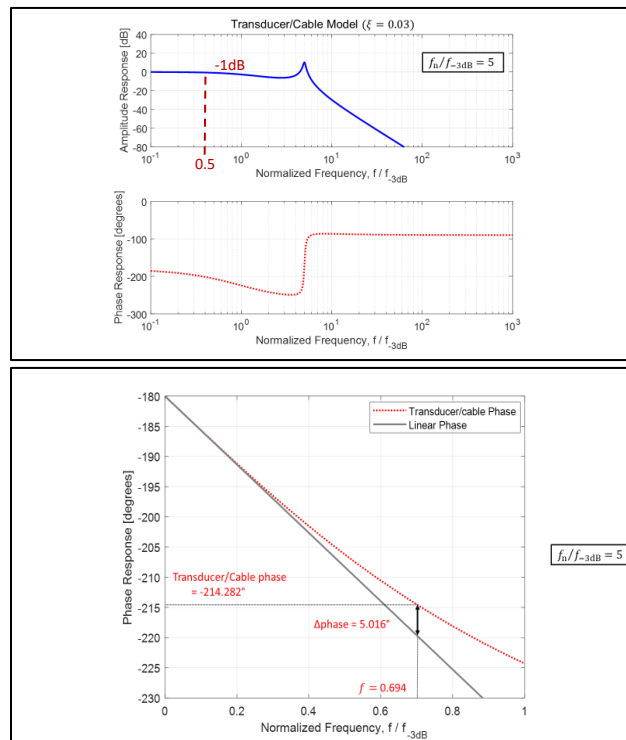


**Figure 5. Idealized Combined Accelerometer/Cable Model (top) and Assessment of Model Phase Nonlinearity (bottom)**

Figure 5 (top) combines the accelerometer model and the cable model of Figure 4. To accomplish this, the individual amplitude responses must be multiplied and the phase responses added. Based on the projection of the initial phase slope in Figure 5 (bottom), 5 degrees phase nonlinearity for the combined model occurs at 0.694  $f_{3dB}$ . For the PCB 3991A-20K example used earlier, this corresponds to about 9.7 KHz (14 KHz x 0.694). However, from Figure 5 (top), -1 dB amplitude attenuation occurs at about 7 KHz (14 KHz x  $\sim$  0.5  $f_{3dB}$ ). Thus, the referenced MIL STD constrains the useable frequency response of the accelerometer/cable combination to  $\sim$  7 KHz (7 < 9.7). Note, the manufacturer's specification for useable frequency response for the 3991A-20 K is 10 KHz (Table 1). Also, of note in this example, the low-pass filtering effect due to the cable attenuates the output signal amplitude at  $f_n = 70$  KHz by 12 dB.

Figure 6 (next) shows that if hypothetically the natural frequency of this accelerometer were increased by a factor of 10 ( $f_n/f_{-3dB} = 50$ ), while the same  $RC = \tau$  lowpass accelerometer/cable time constant was maintained, no improvement in useable frequency response would occur. In addition, the low-pass filtering effect due to the cable attenuates the output signal amplitude at  $f_n$  (now = 10 x 70 or 700 KHz) by 34dB. The output signal amplitude at  $f_n$  would be 10 dB below the static (0 Hz) response of the accelerometer model.

It is not unusual in severe shock for the natural frequency of the MEMS element to be structurally excited and superposed on the desired low frequency signal (below 10 KHz here). The signal attenuation observed at  $f_n$  in both preceding examples ( $f_n/f_{-3dB} = 5$  & 50) has advantages and disadvantages. For example, this attenuation might preclude the linear range of the signal conditioning amplifier from being exceeded at or around  $f_n$ . Signal overrange and/or “clipping” is a nonlinear process resulting in the generation of false data frequencies in the recorded data. Conversely, if the MEMS element is overstressed or breaks, the cause of breakage could be obscured by this signal attenuation at  $f_n$ .

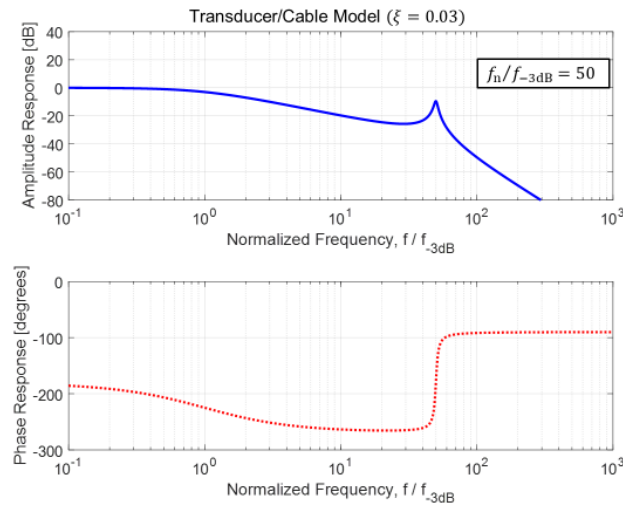


**Figure 6: Idealized Combined Accelerometer/Cable Model  $f_n/f_{-3dB} = 50$**

After modeling the two (2) preceding values of  $f_n/f_{-3dB}$ , a parametric study was performed by varying  $f_n/f_{-3dB}$  continuously, as in Figure 7. Results in Figure 7 clearly show that as  $f_n/f_{-3dB}$  gets below a value of approximately 3, any useable gain in frequency response becomes limited by the 5-degree phase nonlinearity requirement. A conservative value in test planning would be to keep  $f_n/f_{-3dB} > 3$  and limit useable frequency response of the cable/accelerometer system to no more than 0.51 (51%) of  $f_{-3dB}$ .

While cable selection considerations have been discussed before<sup>4</sup> and equations presented, this research represents the first detailed study on the frequency constraints cables place on MEMS accelerometers. The experimental model verification that follows will validate these constraints as well as identify additional limitations posed when considering the cable resistance alone. While all 3 accelerometer models come in the package configurations shown in TABLE 1, other package configurations exist (Figure 8). In Figure 8, the only manufacturer’s specification difference between the 3991 and 3501 (e.g.) in equivalent acceleration ranges is mounting preference.

*\*The contribution of Professor Tristan Tayag, Texas Christian University, in model development and computational validation for the preceding section is gratefully acknowledged.*

## EXPERIMENTAL MODEL VERIFICATION

Three **20 KG** (20,000 G range) accelerometers in the same mechanical configuration as the 3501 (1/4-28 thread) were made available for testing from PCB – one of each model. They are tracked by Model and S/N. The output resistance unique to each accelerometer  $R_{out}$  ( $R_o$ ) is also provided in ohms ( $\Omega$ ).

<b>PCB 3501B1220 KG</b>	<b>S/N 11009</b>	<b><math>R_o = 6543 \Omega</math></b>
<b>Endevco 7270A-20KM4</b>	<b>S/N 11053</b>	<b><math>R_o = 577 \Omega</math></b>
<b>Endevco 7280AM4-20K</b>	<b>S/N 11417</b>	<b><math>R_o = 4674 \Omega</math></b>

The individual calibration sheets provided by the manufacturer with each Model and S/N are available in Appendix A.

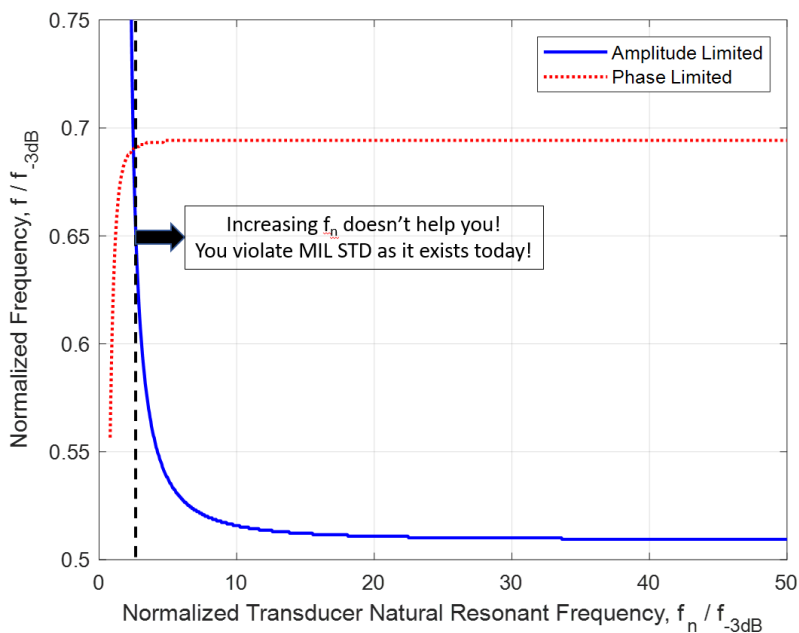


**Figure 7: Limitations in Useable  $f/f_{-3dB}$  As a Function of  $f_n/f_{-3dB}$**



**Figure 8. PCB 3991 (top) and 3501 (1/4-28 mounting thread bottom)**

Each of the three (3) accelerometers was delivered with 10 feet of manufacturer provided integral cable. The cable delivered on the 3501 was the PCB Model 096, which had been reported on previously<sup>4</sup> and was selected as the standard MEMS shock cable for testing. At an appropriate point in an individual test sequence, each accelerometer under evaluation had an additional 153 feet of 096 cable spliced to its existing cable. Any accelerometer/cable time constant ( $RC$ ) determination could then be normalized to the same cable capacitance and illustrate the effect of system  $RC$  product on the maximum useable data content. For this reason, all initial data will be presented as having been acquired through 163 feet of PCB Model 096

cable, which is a close approximation. The 163-foot figure resulted as a byproduct of a request for 150 feet, with 153 feet shipped to splice onto the 10-foot integral cables provided.

With hardware available for testing, numerous issues associated with the influence of the cable impedance must be further understood. Specific issues include:

1. Loss of high frequency data content due to unaccounted filtering effects associated with the cable;
2. Signal attenuation at all frequencies due to cable line resistance;
3. Individuality of hardware:
  - a. The output resistance across the various accelerometer models of interest were noted in the specifications to vary by 26:1;
  - b. The cable capacitance and line resistance vary with cable type, cable length, number of conductors, conductor diameter, and “field” repairs resulting in more than one type of cable spliced to another, and more;
4. In-situ electrical characterization of the cable/accelerometer system’s output frequency capability immediately before initiating any field test.

### DETERMINATION AND VERIFICATION OF APPLICABLE CABLE CAPACITANCE AND SENSOR OUTPUT RESISTANCE

As shown above, the “cutoff” or -3 dB limit of the combined cable/accelerometer MEMS sensing element is controlled by its output resistance  $R$  and cable capacitance  $C$  according to  $f_{-3dB} = (2\pi RC)^{-1}$ . Methods for determining the applicable  $R$  and  $C$  to compute  $f_{-3dB}$  are developed below, along with a procedure to validate the predicted roll-off through direct measurements using standard bench-top instruments. Finally, a method for in-situ, pre-test characterization of actual cable roll-off in a measurement system with a properly equipped signal conditioner is described, based on Precision Filters proprietary *AC Shunt Calibration* technique. Reference 6 (Szary *et al.*) provides additional details to support this section of the report.

#### Determining applicable cable capacitance (C):

A standard 4-wire connection from a MEMS PR shock accelerometer to a signal conditioner is shown in Figure 9. The 4-wire cable connects (+) and (-) excitation supply to the bridge inputs, and the (+) and (-) signal outputs to the signal conditioner’s differential input. The shield of the cable is connected to ground at the signal conditioner and shields the internal conductors from electrostatic noise.

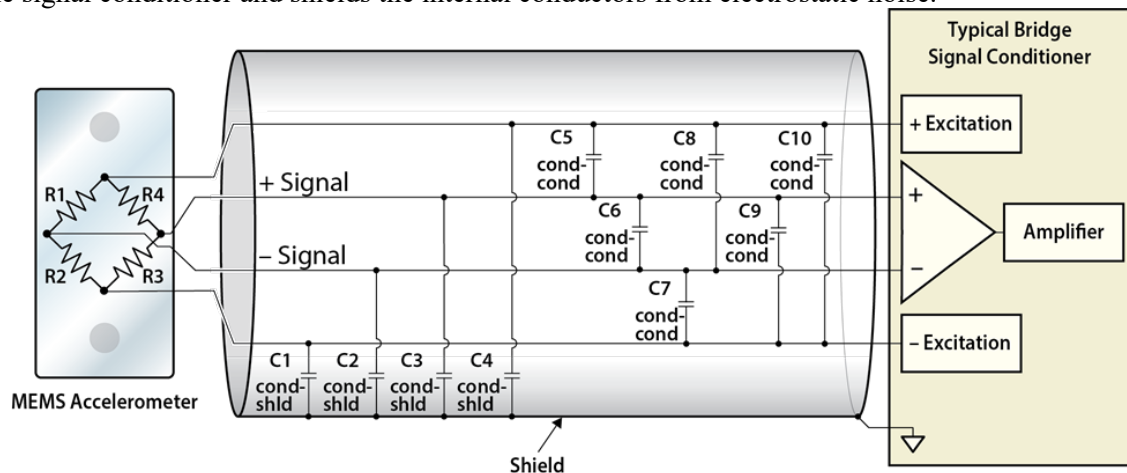


**Figure 9. Diagram of a measurement system with a MEMS sensor, 4-wire cable, and signal conditioner. All conductor-shield and conductor-conductor capacitances are shown.**

To quantify the cable roll-off two key points must be understood:

1. Every conductor within the cable has a deterministic capacitance to the cable shield, denoted here as  $C_{cond-shld}$ . For a properly designed non-paired multi-conductor cable, the assumption is made that all conductor-to-shield capacitances are equal. In Figure 9, these capacitances are numbered  $C_1-C_4$ .
2. Every conductor within the cable also has a deterministic capacitance to every other conductor, denoted here as  $C_{cond-cond}$ . Again, the assumption is made that in a properly constructed non-paired cable the conductor-to-conductor capacitances are equal. In Figure 9, these capacitances are numbered  $C_5-C_{10}$ .

Previous work by Precision Filters<sup>6</sup> describes how to determine correct values for  $C_{cond-shld}$  and  $C_{cond-cond}$  and shows how the model in Figure 9 can be reduced to a single relation for the total cable capacitance,  $C_{total}$ , required for the determination of cable roll-off in a full bridge circuit:

$$C_{total} = C_{cond-shld} + 4C_{cond-cond}$$

### Determining the applicable resistance (R):

The balanced symmetry of the bridge circuit shown in Figure 9 allows analysis of the roll-off on only the (+) signal output, since the roll-off on the (-) signal output will be equivalent. Figure 10 shows a simplified drawing of the (+) signal output from the MEMS accelerometer.

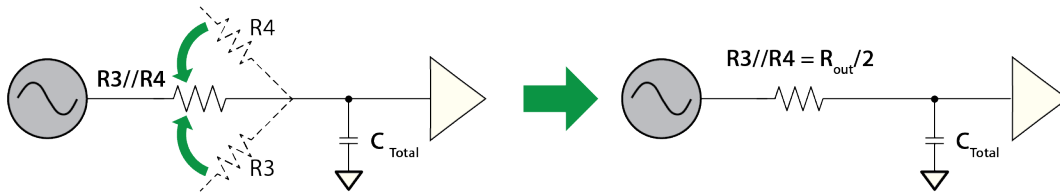


**Figure 10. Simplified model of the bridge circuit (+) signal output in the MEMS accelerometer. The measured output resistance,  $R_{out}$ , reported on manufacturer calibration sheets is related to  $R_3//R_4$  as shown.**

The resistance acting on the cable capacitance  $C_{total}$  is the parallel combination of  $R_3$  and  $R_4$ , commonly denoted  $R_3//R_4$ . As discussed earlier, output resistance varies widely from sensor to sensor due to lot-to-lot variation in sensor production. Fortunately, most accelerometer calibration certificates report an output resistance,  $R_{out}$  that represents the exact measured resistance between the bridge corners for a given accelerometer. As shown in Figure 10, this output resistance equates to twice  $R_3//R_4$ , and thus provides an accurate approximation of the bridge output resistance that can be used to estimate cable roll-off in a full bridge with 4 active arms.

An additional contributor to cable roll-off with low impedance sensors is the series resistance of the cable. In cases where a cable is extremely long or of very small diameter, this series resistance cannot be ignored. Since the cable series resistance is distributed over the entire length of the cable, its effect on cable roll-off cannot be analyzed using the full value as a lumped element at the location of the sensor. Bench-top measurements with different lengths and types of cable have shown that the cable series resistance at the location of the sensor is well-approximated as  $(1/3)*R_{cbl}$ , where  $R_{cbl}$  is the total distributed resistance of each of the two wires. This resistance must be added to  $R_{out}/2$  for an accurate determination of the cable roll-off.

Using values determined for  $C_{total}$  and  $R_{out}$ , our simplified model for the sensor-cable pair can be used to estimate the cable roll-off frequency,  $f_{-3dB}$  (Figure 11). Of note here, while cable inductance does have an effect at higher frequencies, predictions of cable roll-off at  $f_{-3dB}$  and below are shown to be better than 5% accurate even without considering cable inductance. Cable inductance is therefore not included in the analysis that follows.

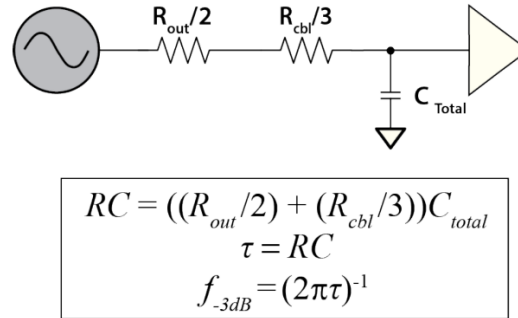


**Figure 11. Summary diagram (top) and formulation (bottom) of the sensor-cable roll-off estimation method. Note that RC is defined as the time constant,  $\tau$ , introduced earlier.**

**Application:**

The methodology outlined above can be used to estimate the -3 dB cable roll-off for any sensor-cable pair. Here cable roll-off is predicted for the three test accelerometers (listed by model, S/N and  $R_0$ ) at the top of page 8. Assumptions are that each sensor is paired with 163 feet of cable: 10 feet of integral 096 low noise 4-conductor cable connected to 153 feet of PCB model 096 extension cable. Capacitance measurements are made in accordance with the methodology developed by Precision Filters<sup>6</sup> and converted to a total capacitance using the method outlined above. The output resistance,  $R_{out}$ , was obtained from factory calibration certificates for each sensor. The cable series resistance was obtained from measurements on the PCB 096 cable (0.42 ohms per foot). The resulting estimates (Predicted  $f_{-3dB}$ ) are summarized in TABLE 2.

**Experimental Verification:**

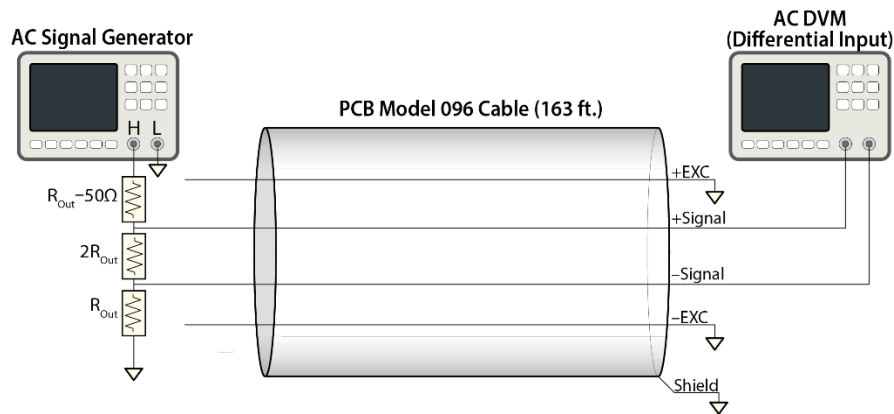


**Figure 12: Bench-top setup used to obtain measurements of sensor-cable roll-off for comparison with values predicted using the model summarized in Figure 11. The procedure is described in more detail in Reference 6.**

To check the accuracy of cable roll-off estimates, the laboratory procedure described by Precision Filters was used to obtain measurements of roll-off for each sensor-cable pair in Table 2 (Figure 12). The setup paired the same type and length of PCB cable with resistors that matched the output resistance of each MEMS sensor.

For this setup to accurately represent actual test conditions, the following requirements must be met:

- The cable shield is grounded so as to be equivalent to the run-time condition.
- (+) and (-) excitation lines are connected to ground at the signal conditioner side of the cable to simulate the same low impedance to ground as the constant voltage excitation supply.
- A differential signal is applied to (+) signal and (-) signal wires through a differential attenuator made up of discrete resistors equal to  $R_{out}$  and  $2*R_{out}$  where  $R_{out}$  is the output resistance from the calibration certificate of the selected accelerometer.
- If the signal generator has non-zero output impedance (typically 50 ohms, as shown in Figure 12), this resistance should be taken into account by subtracting from the upper bridge-simulating resistor for improved accuracy of the roll-off measurement.

With these requirements satisfied, the  $f_{-3dB}$  frequency can be determined by sweeping the signal generator from 100 Hz to 100 kHz (Figure 13). The results ( $Measured f_{-3dB}$ ) are given in TABLE 2. Measured values for each sensor differ from the predicted values by less than 2%.

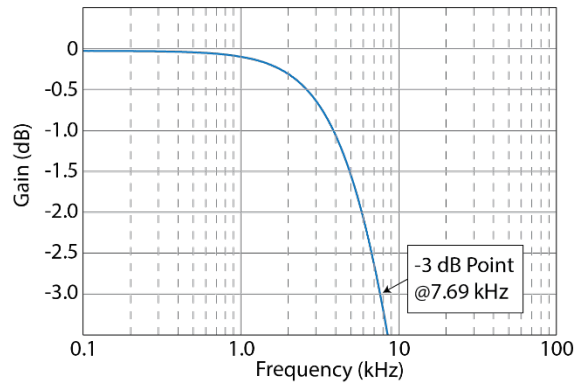


**Figure 13. Results of the bench-top experiment described in Figure 12 for the PCB 3501**

Sensor Model	Sensor SN#	Sensor $R_{out}/2$ (ohms)	Cable $(1/3)*R_{cbl}$ (ohms)	Cable $C_{total}$ (pF)	Predicted $f_{-3dB}$ (kHz)	Measured $f_{-3dB}$ (kHz)
PCB 3501B1220KG	11009	3,272	22.8	6,152	7.85	7.69
Endevco 7270A-20KM4	11053	289	22.8	6,152	83.0	82.7
Endevco 7280AM4-20K	11417	2,337	22.8	6,152	11.0	11.0

**TABLE 2. Predicted and measured values for the sensor-cable roll-off ( $f_{-3dB}$ ) of three MEMS accelerometers. Note that  $R_{out}$  values for each sensor are taken directly from the manufacturers' calibration certificates.**

## AC Shunt Calibration for In-situ Cable Roll-off Determination

The experimental verification of cable roll-off predictions using the method described above is often impractical for measurements in the field. Common practice is to specify an accelerometer with a predetermined length of lead wire that is integral to the delivered accelerometer assembly. Often the lead wire installed by the manufacturer is very fine 32-36 gage wire. Cutting and re-splicing this wire for the purpose of conducting the above measurement would be undesirable. Additionally, conducting a sensitive measurement in a harsh environment with specialized equipment is logistically difficult. For this reason, Precision Filters has developed a proprietary technology called *AC Shunt Calibration*<sup>10</sup> which enables the direct measurement of cable roll-off from the convenience of the instrumentation room. In AC shunt calibration, an AC current is injected into the  $R_1/R_2$  bridge corner (Figure 14). This current interacts with the actual output resistance of the bridge corner to produce a sensor-based test signal  $V_{test}$  that is equal to  $I \cdot R_{out}/2$ . As the frequency of the test signal is increased, the interaction of the actual cable capacitance and the sensor's actual output resistance produces a very similar frequency response as that produced by the MEMS element within the active sensor.

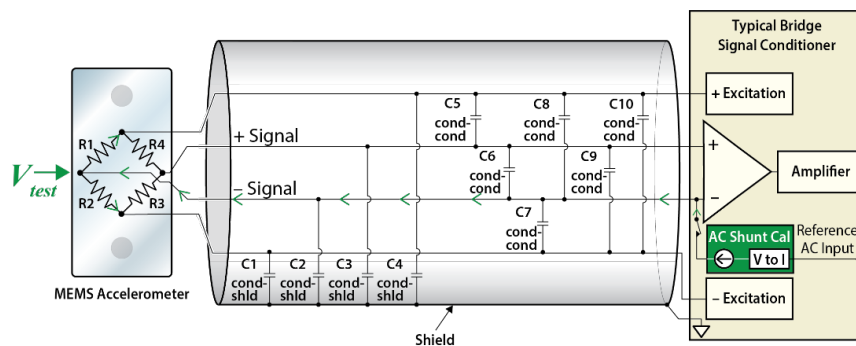


**Figure 14. Diagram of the measurement system shown in Figure 9 configured for AC Shunt Calibration. The simulated test signal generated within the MEMS sensing element is  $V_{test}$ .**

The Precision Filters AC Shunt Calibration technique<sup>10</sup> was used to measure the cable roll-off for the same sensor-cable pairs in Table 2. The results (Figure 15) are consistent with the predicted and laboratory measured values. For comparison, the red traces in the graphs show the dramatic difference in cable response with only the 10 feet of factory installed cable.

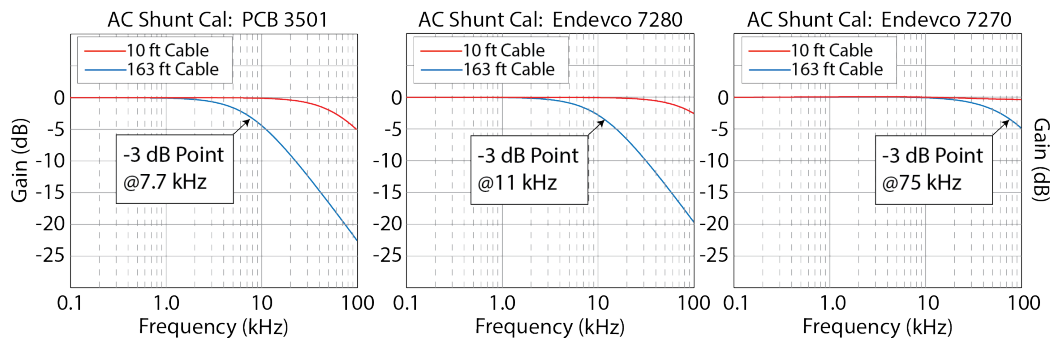


**Figure 15. Results of AC shunt calibration tests on the sensor-cable pairs showing good agreement with data summarized in TABLE 2.**

## MECHANICAL SHOCK TEST VERIFICATION

As supplied (and verified by their specifications in TABLE 1), all three (3) of the above MEMS accelerometer models were certified to have a flat frequency response to a minimum of 10 KHz. Applying the results and discussion associated with Figure 7, the 163 feet of cable constrain the maximum useable frequency response of the accelerometers to 51% of their -3dB frequencies. Calculating 51% of the -3dB frequencies in Figure 15 (7.7 KHz, 11 KHz, and 75 KHz)] results in a maximum upper frequency limit of acceptable performance of 3.9 KHz, 5.6 KHz, and 38 KHz respectively. These maximum limits are based on the experimentally verified -3dB frequencies and the requirements of MIL-STD-810H. If the default frequency requirement of 10 KHz is accepted, two (2) of the accelerometers are immediately disqualified from consideration for shock application. The resistive output impedance of the MEMS element, interfaced to the electrical impedance of the cable, controls this *maximum* upper frequency limit of performance.

A question that should arise is: What if a shorter length (less than 163 feet) of the 096 cable had been used? The frequency response would be improved for each of the individual accelerometers. However, again note that among these accelerometer models, the output resistance in the extreme varies by a factor of 26:1. If another accelerometer of any model that by chance possessed a higher  $R_{out}$  were acquired, more frequency response might be lost than would be gained, even with a shorter length of cable. Dependent on cable type, a different cable might improve or lessen this maximum frequency limit.

While the specific length of cable tested was arbitrary, the need for long cables or cable extensions can best be illustrated (Figure 16 below) by the importance, expense, and hazards associated with severe shock tests, particularly at the systems level. To achieve reliability in complex systems, a finite number of full-scale system level shock tests are performed. The localized shock input to critical components that must survive and function during these tests is measured. Once system level testing enables determination of the input to these components, reliability at the systems level can subsequently be maintained through certification testing at the component level. All component testing is notably only as good as the system level shock measurements upon which it is based.



**Figure 16 Example of Systems Level Testing**

Assuming the electrical bench testing results of Figure 15 are correct, under mechanical shock the time-domain performance of the accelerometers should improve across the specific accelerometers/models from left to right. A laboratory shock capability was constructed to evaluate this premise. The design requirements that this laboratory shock capability had to satisfy were:

1. Capable of generating highly repeatable shock pulses;
2. Capable of generating shock pulses with significant frequency content to 10 KHz while still being “rich” in frequency content above that frequency;

3. Capable of generating significant shock amplitudes (multiple 1000s of Gs) to provide an adequate signal level to measure while not overranging or damaging the accelerometers (*note*: All MEMS accelerometers evaluated produced about 50 mV output at 5,000 G);
4. Capable of providing identical time/frequency signatures concurrently to both a reference accelerometer and the specific MEMS accelerometer being compared. The reference accelerometer selected was a 350D02 Mechanically-Isolated & Electrically Filtered ICP® accelerometer;<sup>1,2</sup>
  - Its Full Scale Range of 50 KG would assure its survivability;
  - Although higher in Full Scale Range, its sensitivity was still 10 times greater than the test MEMS units;
  - Its increased sensitivity allowed its frequency response to be verified under vibration calibration as flat (essentially constant) and plotted to 10 KHz as displayed in Appendix A (A.2).

A versed sine or haversine pulse is frequently specified for component shock verification. Fourier Transforms were iteratively calculated to determine that a 100 to 125 microsecond duration haversine shock pulse would contain significant spectral content to 10 KHz enabling test to test comparison. Based on this analysis, a ballistic type pendulum was designed where two (2) identical, large, chrome-steel ball bearings on rigid moment arms would be rotated through equal angles and impacted in a co-linear manner. The controlled geometry of the bearings assured symmetry of impact. Their mechanical properties allowed them to remain undamaged during repeated impacts (Figure 17).

To extract rigid body motion from the bearings, the following minimum Design Constraints were placed on the bearings:

1. Their lowest resonant frequency had to be at or above 50 KHz;
2. Their mass had to be large compared to that of their rigidly attached accelerometers; and
3. The bearings themselves had to be isolated from the dynamics of their moment arm.
  - a. An elastomeric interface between the bearings and the moment arm accomplished this.

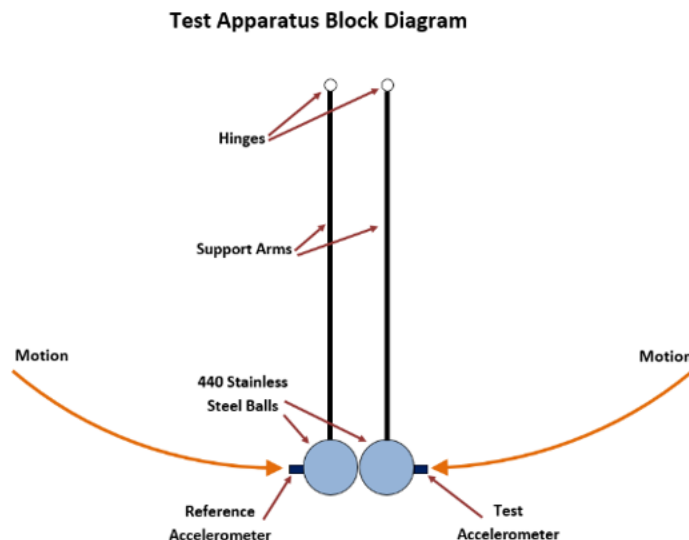


**Figure 17. Illustration of the Ballistic Pendulum Used in Shock Testing**

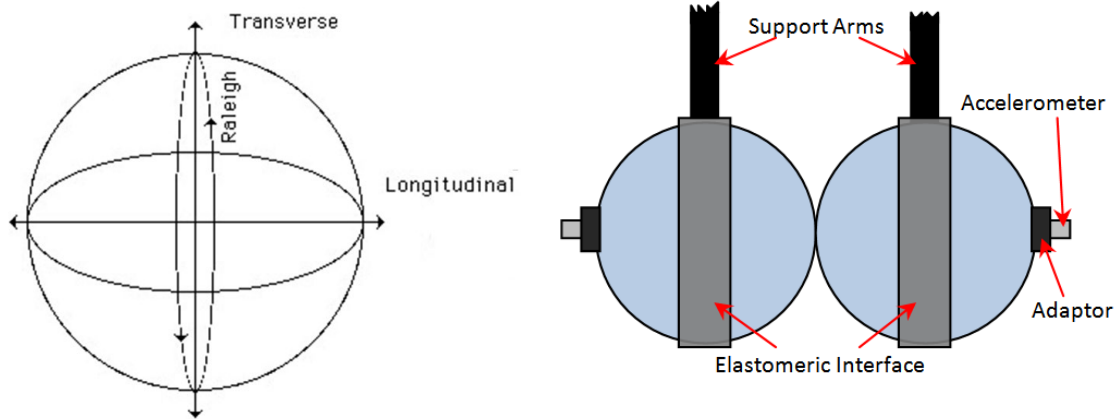


**Figure 18. Wave Propagation in Solid Sphere (left). Longitudinal shown is P-Wave. Accelerometers on bearings (right) are rigidly mounted and elastomeric mounts that isolate the bearing from their support arms are pictorially shown.**

Based on classical theory of wave propagation in elastic spheres,<sup>7</sup> a 2.0-inch diameter steel ball bearing would have a round-trip transit time for its P or Longitudinal wave (Figure 18) of 0.0000204 seconds. This corresponds to a resonant frequency of ~50 KHz. A structure can be considered a “rigid” body to one-fifth of its lowest resonant frequency (e.g., 50 KHz/5 = 10 KHz). Thus, the 2-inch diameter bearing should satisfy the preceding Design Constraint #1. The weight of each ball bearing is 527 grams, the adapter and accelerometer combined is 3.2 grams. This satisfies Design Constraint #2 (527 >> 3.2 grams). Design Constraint #3 will be shown to be satisfied by the following qualification of the pendulum employed in the ‘Ballistic Pendulum Qualification Testing’ section of this report. The remainder of testing performed employs mechanical shock testing specifically to validate TABLE 2 and Figure 15. The following comments apply to all testing:

- ✓ The signal conditioning amplifiers used in testing were certified to have a -3dB frequency of 250 KHz. When testing the 7270A-20KM4, an amplifier with a -3dB frequency of 500 KHz was used. All acquired data were digitized at a rate of 1 million samples/second.
- ✓ The term **Wideband** in the context used below implies the only frequency limitation in the data are those imposed by the cable between the accelerometer and the signal conditioning.
- ✓ The term **Filtered** in the context used below denotes that an eighth-order linear-phase analog filter (PFI LP8P) was introduced in the front end of the signal conditioning. The filter was configured to have 1 dB attenuation at 10 KHz\* and subsequently attain a slope of -160 dB/decade (48 dB/octave). Its purpose was both to satisfy the signal conditioning requirement of MIL-STD-810H and enable time domain data comparison against the Reference Sensor to 10 KHz. See Appendix B for the PFI LP8FP filter specifications.<sup>9</sup>

\* This would be a reasonable filter setting with an assumption that there was no additional attenuation due to cable roll-off.

## Ballistic Pendulum Qualification Testing

The intent of this testing was to assess the capability of the ballistic pendulum to deliver concurrent and repeatable deceleration shock pulses to both captured ball bearings over a frequency span up to and including 10 KHz. A PCB Model 350D02 accelerometer was rigidly adapted to the surface of each bearing, and both pulses were recorded on impact. 10 milliamps of current was provided to the ICP circuit of each accelerometer. Again note, the calibration data in Appendix A.2 showed both accelerometers have “flat” or constant frequency response to 10 KHz. As in all bench testing, care was taken not to tightly coil or kink the cables. 350D02 S/N 63666 was designated as the Reference Sensor and its response is indicated *red* in all comparative recorded shock data plots.

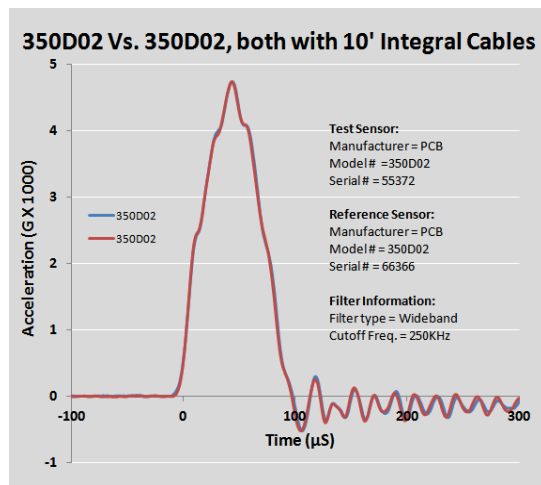
Note: To account for the time delay caused by the 350D02’s internal 2 pole filter, its output time axis was shifted 10 µseconds to properly align it with all comparative tests sensor data plots below (Plots 4-18).

[Plot #1] Wideband data were recorded multiple times, and what looks like a single trace is really two accelerometer traces (red and blue) on top of one another. If we look between the 200 and 300 µsec time markers we see approximately 5 cycles of a sine wave corresponding to a frequency of 50 - 53 KHz. Since the two accelerometer signatures correlate, this could verify the validity of the 50 KHz calculation of the resonant frequency of each ball bearing. Accelerometer performance cannot be verified traceable to national standards above 20 KHz.

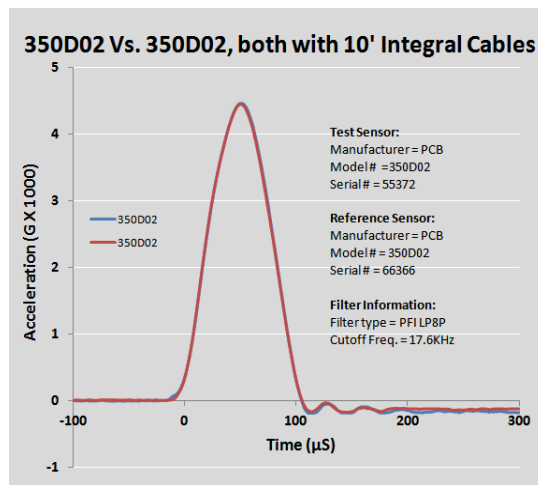
[Plot #2] The PFI LP8P Filter was inserted into the signal path and testing was repeated. Excellent correlation in the time-domain was noted. Both acceleration traces again lay on top of one another. The “ripple” after the pulse termination is understood and is an artifact of the filter.

[Plot #3] Observe that the Fourier Spectra magnitude of the pulses in plot #2 superpose almost exactly to 10 KHz. Above 10 KHz the analog filter progressively contributes to the attenuation of the two spectra. Significant frequency content to 10 KHz (and above) was achieved in testing (~ 100 µsec pulse width). Note, all testing displayed in plots #1, #2 and #3 was performed with only the 10 feet of attached cable supplied by the manufacturer.

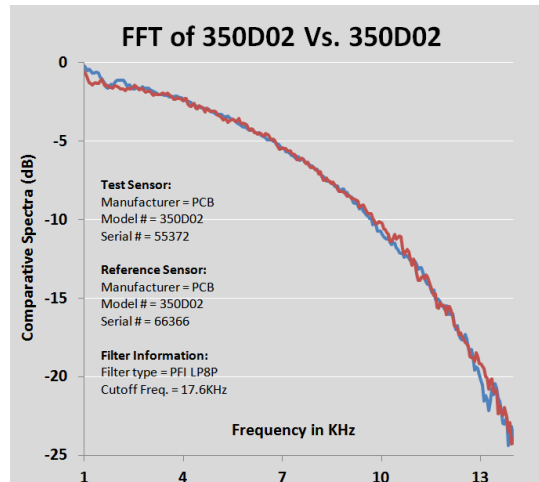
Conclusion: *All ballistic pendulum test system design goals were achieved. Performance assessment of the various MEMS accelerometer models could proceed.*



Plot #1



Plot #2



**Plot #3**

### **7270A Performance Assessment**

Accelerometer Rout = 577 Ohms, Cable Length 10' and 163'

Previous discussion based on Figure 15 concluded that the specific 7270A-20KM4 supplied (Output Resistance of 577Ω) should satisfy the 10 KHz requirement of the MIL-STD both with and without the additional 153 feet of cable. Test results follow:

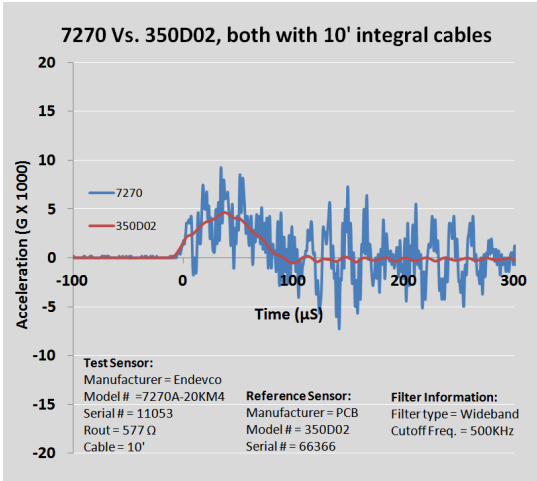
[Plot #4] Outcome of shock testing with 10 feet of cable and Wideband recording are shown. Note the higher indicated G output and frequencies in the signature (blue) of the 7270A.

[Plot #5] A portion of the recorded signal between 50 and 100 μsec is time expanded. The observed 20 cycles of oscillation divided by the 50 μsec time interval calculate to approximately 400 KHz. As a plausible explanation, the nominal resonant frequency of this model/range was specified to be 350 KHz (see TABLE 1).

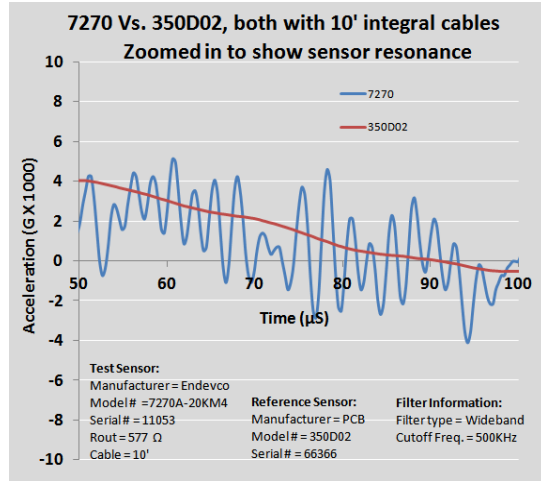
[Plot #6] The PFI LP8P filtered data shows excellent correlation in the time domain indicating both Test and Reference Sensor agreement to 10 KHz.

[Plot #7] Recorded Wideband, note that the 153 feet of added cable causes the 400 KHz resonance to be eliminated from the data. The input signal to the accelerometer cable is closely approximated by Plot #4, but the complex impedance of the cable eliminated any indication that the resonant frequency of the accelerometer has been excited. Note that a modulation frequency is visible in Plot #7 and, under closer examination, is slightly apparent in Plot #4. This modulated or beat\* frequency is shown here to be about 10 KHz and is the difference (explained later) between two other frequencies  $|f_1 - f_2|$ .

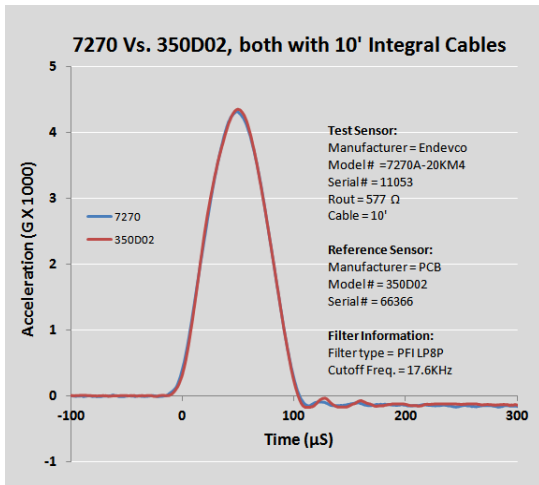
[Plot #8] Continuing comparison shock testing with the added 153 feet of cable shows the Test and Reference Sensors both correlate in time and, therefore frequency to 10 KHz. The PFI LP8P filter was again inserted into the signal path. The complex impedance of the cable has not constrained acquisition of accurate 10 KHz shock data.



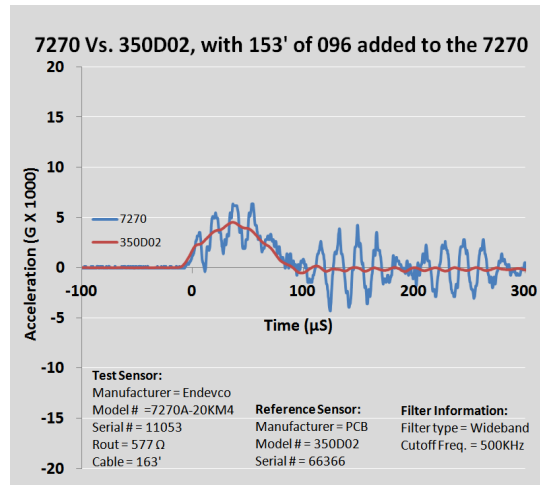
**Plot #4**



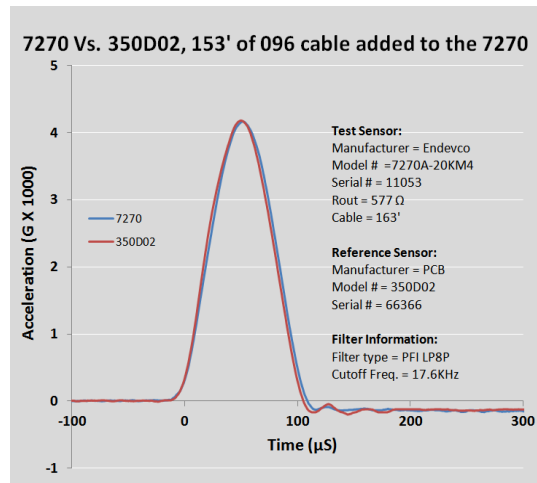
**Plot #5**



**Plot #6**



**Plot #7**



**Plot #8**

## 7270A Supply Voltage Assessment

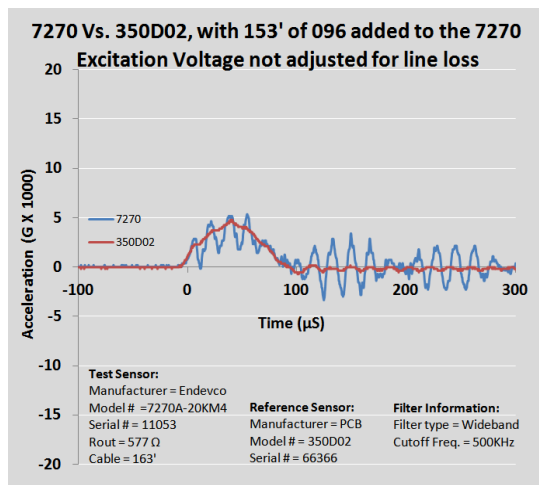
Accelerometer Rout = 577 Ohms, Change in Cable Length 153'

In all prior testing, 10 VDC Voltage was supplied to the Test Sensor. The 10 VDC supply voltage was measured as it was in the original calibration process, at the input to the 10-foot cable. If additional cable was attached, the 10VDC was still controlled at the splice connecting the two cables, i.e. at the same location.

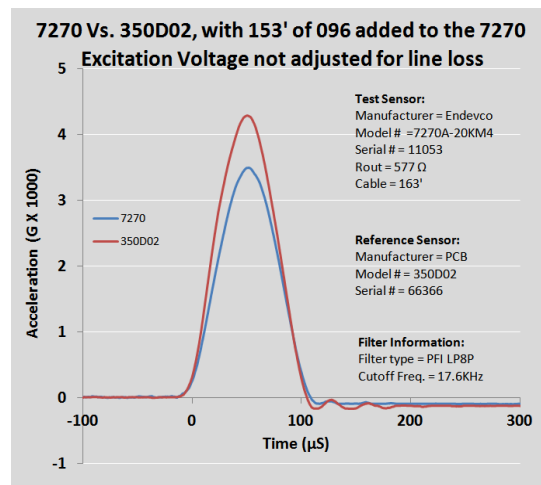
[Plot #9] The shock pulses displayed were recorded Wideband with the 10 VDC supply to the 7270A controlled at the excitation source, as opposed to the splice where the additional 153 feet of added 096 cable was connected. When filtered previously these shock pulses superposed. Testing in plot #10 below assesses if this superposition still exists.

[Plot #10] When Filtered, both pulses are observed to be similar in waveform, but the Test Sensor is 18% smaller in amplitude. This attenuation occurred since the 10 VDC supply voltage was controlled at the source of the 153' of additional cable as opposed to the location where it was spliced. 12.2 VDC at the cable source, in this instance, would have resulted in 10 VDC at the splice. The resistive and reactive impedance components of the cable still mitigate the higher frequencies from the Test Sensor (7270A). The resistance of the cable alone decreases the DC supply voltage to the Test Sensor uniformly lessening its output - *in this case by 18%!*

Conclusion: *The lower resistance of the 7270A (Output Resistance of 577Ω in this case) results in less frequency attenuation due to complex cable impedance. However, this lower resistance makes it more susceptible to line loss decreasing its supply voltage.*



Plot #9



Plot #10

## 7280AM4 Performance Assessment

Accelerometer Rout = 4674 Ohms, Cable Length 10' and 163'

Previous discussion based on Figure 15 concluded the specific 7280A supplied (Output Resistance of 4674  $\Omega$ ) should satisfy the 10 KHz requirement of the MIL-STD without (but not with) the additional 153 feet of cable. Test results follow:

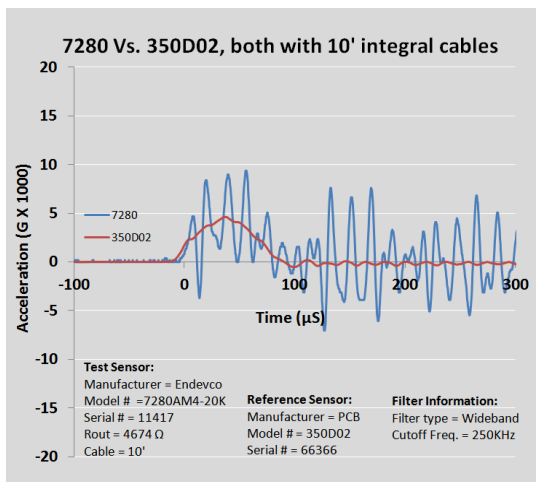
[Plot #11] The Wideband shock pulse comparison with 10 feet of cable is shown. TABLE I specifies the resonant frequency of the 7280A to be 100 KHz. The Test Sensor frequency observed in the record may be a bit lower than this value, but within tolerance.

[Plot #12] As predicted, the PFI LP8P Filtered data (10 feet of cable) shows excellent correlation in the time domain indicating both Test and Reference Sensor agreement to 10 KHz.

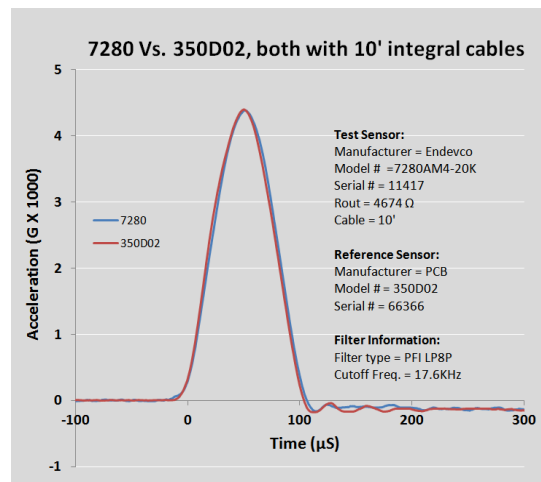
[Plot #13] The Wideband shock pulse comparison with the addition of 153 feet of cable is shown. Note that the Test Sensor resonance was severely attenuated. The input signal to the accelerometer cable is closely approximated by plot #11, but the complex impedance of the cable has greatly attenuated the resonant frequency response. The supply voltage had been increased to 10.27 VDC to account for resistive line loss. The higher resistance of the 7280A vs the 7270A required a lesser supply voltage increase.

[Plot #14] Continuing comparison shock testing with the added 153 feet of cable shows the Test and Reference Sensors do not correlate in time and, therefore, not in frequency content, to 10 KHz. The PFI LP8P filter was again inserted into the signal path. The complex impedance of the cable has constrained acquisition of adequate 10 KHz shock data. The reduced amplitude and time-shifted Test Sensor pulse peak, along with its increased pulse duration, are directly attributable to the high frequency RC filtering of the cable/sensing element combination.

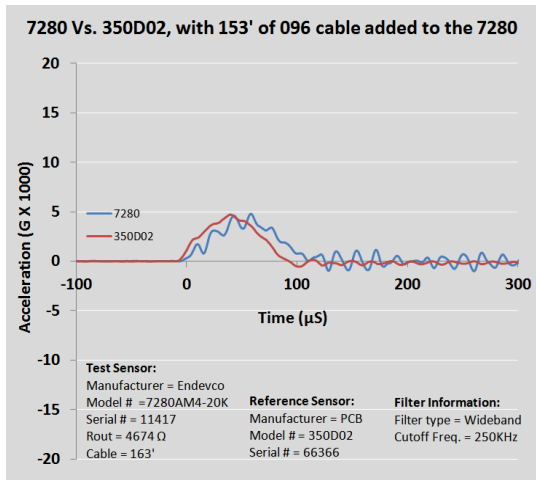
Conclusion: *The higher resistance of the 7280A (Output Resistance of 4674  $\Omega$  in this case) results in increased high frequency attenuation due to the complex cable impedance. Conversely, this higher resistance makes it less susceptible to resistive line loss decreasing its supply voltage.*



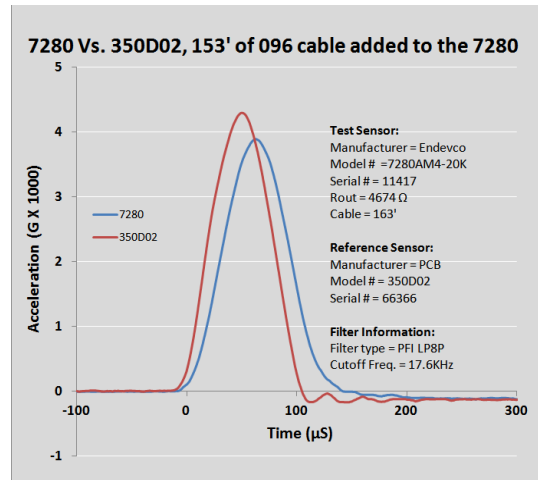
Plot #11



Plot #12



**Plot #13**



**Plot #14**

### **3501B Performance Assessment**

#### **Accelerometer Rout = 6543 Ohms, Cable Length 10' and 163'**

Previous discussion based on Figure 15 concluded the specific 3501B supplied (Output Resistance of 6543 Ω) should satisfy the 10 KHz requirement of the MIL-STD without (but not with) the additional 153 feet of cable. Test results follow:

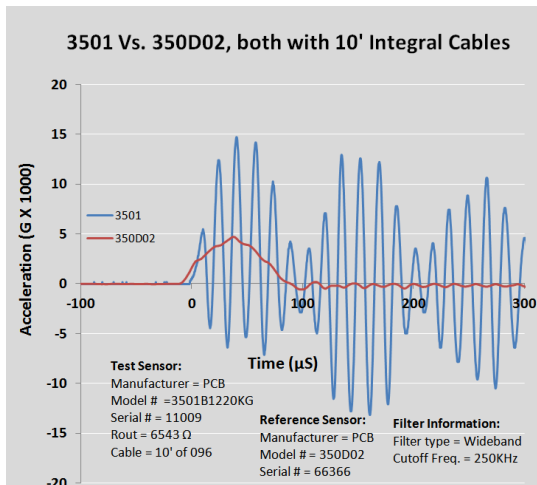
**[Plot #15]** The Wideband shock pulse comparison with 10 feet of cable is shown. TABLE I specifies the resonant frequency of the 3501B to be > 60 KHz. The Test Sensor frequency observed in the record is just slightly over this value (6+ cycles in ~ 100 µsec). Note again the beat\* frequency | f<sub>1</sub>-f<sub>2</sub> |.

**[Plot #16]** As predicted, the PFI LP8P filtered data (10 feet of cable) shows excellent correlation in the time domain indicating both Test and Reference Sensor agreement to 10 KHz.

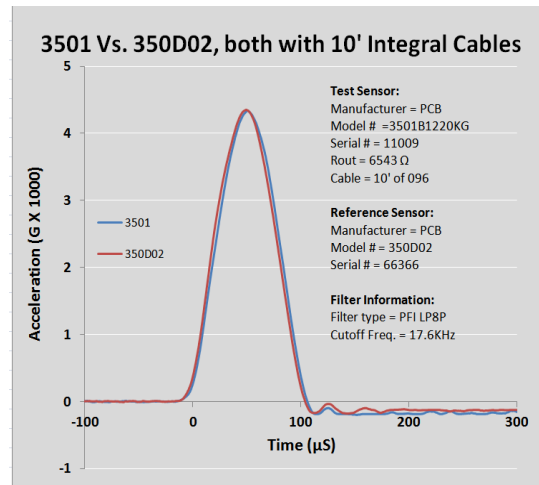
**[Plot #17]** The Wideband shock pulse comparison with the addition of 153 feet of is shown. Note that the Test Sensor resonance was severely attenuated. The input signal to the accelerometer cable is closely approximated by plot #15, but the complex impedance of the cable has attenuated the resonant frequency response by 4:1. The supply voltage had been increased to 10.21 VDC to account for resistive line loss. The higher resistance of the 3501B vs the 7280A vs the 7270 A required the least supply voltage increase.

**[Plot #18]** Continuing comparison shock testing with the added 153 feet of cable shows the Test and Reference Sensors do not correlate in time and, therefore, not in frequency content, to 10 KHz. The PFI LP8P filter was again inserted into the signal path. The complex impedance of the cable constrained acquisition of adequate 10 KHz shock data. The reduced amplitude and time-shifted Test Sensor pulse peak, along with its increased pulse duration, are directly attributable to the high frequency RC filtering of the cable/sensing element combination. The highest degree of time domain distortion correlates with the predictions of Figure 15

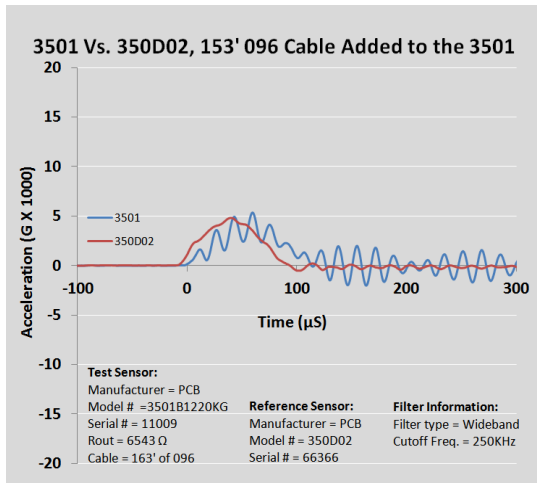
**Conclusion:** *The higher resistance of the 3501B (Output Resistance of 6543 Ω in this case) results in the greatest high frequency attenuation due to the complex cable impedance. Conversely, its higher resistance makes it the least of the 3 Test Sensors tested susceptible to resistive line loss decreasing its supply voltage.*



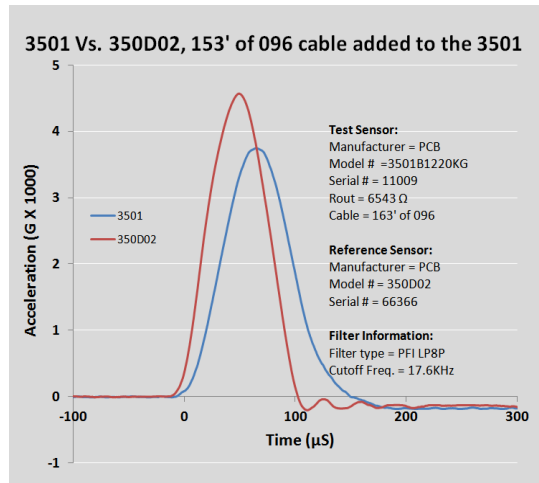
**Plot #15**



**Plot #16**



**Plot #17**



**Plot #18**

*\*note. The plots display a 10 KHz modulation in the Wideband data. The fact that it is present for all three MEMS sensors indicates that it is caused by a higher structural resonance in the bearing/mount assembly (see Figure 17). With a bearing resonance of 50 KHz, a second structural resonance of 60 KHz would create this beat frequency or modulation | 60-50|. Following this logic, this could explain why the resonant frequency (~ 60 KHz) of the 3501(see Plot #15)] is accentuated. This discussion is provided only to provide clarity to the data. The beat frequency is irrelevant to the preceding analysis.*

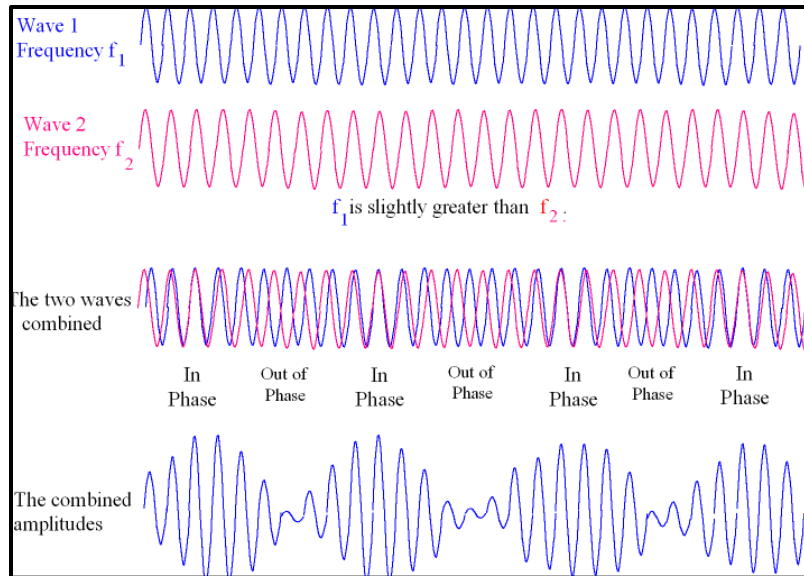


**Figure 19. Explanation of a Beat Frequency**

## OTHER OBSERVATIONS

### Not all cables are created equal

Cable properties can vary significantly from model to model due to differences in: conductor diameter, type, number, and material; jacketed coating material and thickness; shielding material (braided copper, aluminum, and nickel as well as foils) and thickness (single or double shielded); and conductor weaving (straight wire or twisted).



**Figure 20. Examples of different cable types.**

Moreover, the properties of a hybrid cable – constructed by splicing two different cables to achieve a longer run – can vary significantly along its length (see Figure 3). While each aspect of cable design has an intended purpose, their combined effect on the electrical characteristics that determine cable roll-off is less clear. To illustrate, we compare the effect of three different cables, each a 150 ft parallel 4-wire braided shield sequentially spliced onto the PCB 3501B (SN# 11009 as described in TABLE 2), on the frequency response of the cable-sensor pair.

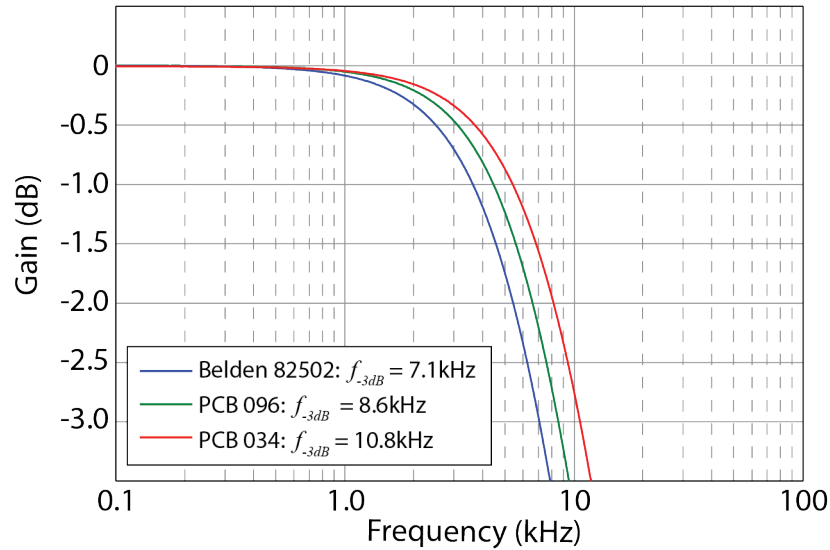


**Figure 21. Variation of cable roll-off using the PCB 3501B (SN#11009 as described in TABLE 2) accelerometer and 150 feet of various cable types.**

To understand the large variation in minus 3dB frequency ( $f_{-3dB}$ ) in Figure 21, the electrical characteristics relevant to cable roll-off are tabulated below (TABLE 3) for each cable type along with the expected roll-off predicted by the equation in Figure 11. The closeness of the predicted roll-off to measured values lends support to the methodology of reference #6 and reinforces the notion that *not all cables are created equal*.

Cable Type	Cable $C_{total}$	Cable Series Resistance	Predicted $f_{-3dB}$ (PCB 3501 $R_{out}/2=3,272\Omega$ )	Measured $f_{-3dB}$
Belden 82502	45.9 pF/ft	0.024 $\Omega$ /ft	7.06kHz	7.1kHz
PCB 096	37.7 pF/ft*	0.420 $\Omega$ /ft	8.55kHz	8.6kHz
PCB 034	28.1 pF/ft	0.293 $\Omega$ /ft	11.5kHz	10.8kHz

**TABLE 3. Cable electrical characteristics applied to the equation of Figure 11 and resultant predicted and measured results.**

*\*Note: Graphite matrix in 096 cable, used to minimize triboelectric noise,<sup>4</sup> slightly increases conductor to shield capacitance while virtually eliminating conductor to conductor capacitance.*

Having established agreement to actual measured response, the calculations of Figure 11 can be extended to infer useful information and guide the test planner to make key decisions in sensor, cable, and logistical issues. TABLE 4 charts the maximum frequency achievable to limit cable roll-off to -1dB for various lengths of these same cables with each of the sensors described in the top of page 8. Alternatively, TABLE 5 charts the maximum allowable cable length (ft) for -1dB cable roll-off at 10 kHz for these sensor/cable pairs.

<b><i>F</i>(max) for -1dB Cable Roll-Off (kHz)</b>									
Cable Type	Cable length = 50 ft			Cable length = 100 ft			Cable length = 150 ft		
	PCB 3501*	Endevco 7270*	Endevco 7280*	PCB 3501*	Endevco 7270*	Endevco 7280*	PCB 3501*	Endevco 7270*	Endevco 7280*
Belden 82502	10.8	122	15.1	5.40	61.0	7.56	3.60	40.6	5.04
PCB 096	13.1	145	18.3	6.55	71.0	9.15	4.35	46.2	6.08
PCB 034	17.6	196	24.6	8.79	96.5	12.3	5.85	63.3	8.18

**TABLE 4. *F*max (kHz) based on -1dB cable roll-off for various cable/sensor pairs.**

*\*Note: refers only to specific sensors described on top of page 8.*

<b>Max Cable Length for &lt; -1dB Roll-Off @10kHz (ft)</b>			
Cable Type	PCB 3501*	Endevco 7270*	Endevco 7280*
	Belden 82502	53	600
PCB 096	65	580	91
PCB 034	87	785	122

**TABLE 5. Maximum cable length (ft) for -1dB cable roll-off at 10 kHz for various cable/sensor pairs. *\*Note: refers only to specific sensors described on top of page 8.***

**Cable Series Resistance:**

In addition to cable roll-off, the cable series resistance related to IR drops on the sensor excitation wiring must be accounted for. The low-mass cabling required for shock accelerometers necessarily consists of small gage (AWG), high-resistance wire. Depending on the ratio of cable resistance to the input resistance of the accelerometer, the IR drop on the excitation wiring could reduce the excitation delivered to the sensing element, causing a reduction in overall sensor sensitivity. Unlike cable roll-off that is only apparent at higher frequencies, reduced sensitivity due to IR drops in the excitation wiring affects all data frequencies. Reputable sensor manufacturers are aware of this desensitization and clearly state that sensor sensitivity presented on a calibration certificate assumes proper excitation at the signal conditioner end of the sensor’s integral cable (i.e., IR drops of the integral cable are accounted for). If additional cable length is added to the factory provided integral cable, the test planer must guarantee proper excitation at the location of the splice. The roll-off measurements presented in Figure 21 were taken while maintaining proper 10V excitation at the location of the splice using a calibrated DVM. TABLE 6 shows the reduced sensitivity that would be expected if the same sensor/cable pairs summarized in TABLES 4 and 5 were employed without correcting the excitation at the location of the splice.

<b>Sensor desensitization caused by cable resistance (%)</b>									
Cable Type	Cable length = 50 ft			Cable length = 100 ft			Cable length = 150 ft		
	PCB 3501*	Endevco 7270*	Endevco 7280*	PCB 3501*	Endevco 7270*	Endevco 7280*	PCB 3501*	Endevco 7270*	Endevco 7280*
Belden 82502	0.0	0.4	0.1	0.1	0.8	0.1	0.1	1.2	0.2
PCB 096	0.7	6.9	0.9	1.3	12.9	1.8	2.0	18.1	2.6
PCB 034	0.5	4.9	0.6	0.9	9.3	1.2	1.4	13.4	1.9

**TABLE 6. Sensor desensitization vs extension cable length without excitation correction at the splice. *\* Note: refers only to specific sensors described on top of page 8.***

It should be noted that if the low-impedance 7270 is selected to drive the capacitance of the long cable for optimal roll-off response, a nominal 18% desensitization error at all frequencies will occur. This tradeoff between improved frequency response (requiring low sensor resistance) and low sensitivity to cable series resistance (requiring high sensor resistance) represents the conflicting requirements, which is the unfortunate trade space the test planer of shock measurement is forced to negotiate. Thankfully, if the decision is made to extend cable frequency response by using low resistance sensors, methods exist to mitigate the potentially large desensitization errors. These methods are described below:

- 1) As was done for the measurements presented in this report, the excitation voltage at the splice can be measured with a DVM. The output of the excitation supply can then be manually increased as necessary until the voltage at the splice is correct. This method is acceptable as long as additional errors caused by resistance changes due to varying temperatures are within acceptable limits.
- 2) The resistance of the excitation wire can be estimated by cable manufacturers' published specifications. This total resistance can be used against the sensors input impedance to calculate the IR drop on the extension wire. Excitation can then be increased by this nominal amount. With relatively high-gage, low-resistance extension wire or when temperature changes in the test environment are known to be minimal, this technique may provide acceptable results. However, care must be taken to ensure that published specifications for cable resistance are accurate and valid for the cable temperature at test time.
- 3) The "Remote Sense" feature of high-performance bridge conditioner front ends uses an additional set of wires to control the excitation actually delivered to the bridge element or any predetermined location along the bridge wiring. The excitation supply automatically and continuously adjusts the excitation to maintain the correct level at the point where the additional "excitation sense" lines are connected to the primary excitation lines. If a 6-wire connection is possible from the splice location to the signal conditioner, then the remote sense method is preferred since it allows for precise and continuous control at all operating temperatures. The 6-wire remote sense technique is by no means a new or novel one, A description of the remote sense technique was documented as long ago as 1964 in the Tech note titled "*System Considerations for Bridge Circuit Transducers*," written by Peter R. Perino for Statham instruments<sup>8</sup>. For details on how to determine total cable capacitance and roll-off for a 6-wire section of a hybrid (spliced) cable, see Szary *et al.*<sup>6</sup>

### **Issues created by large variation of sensor characteristics within the same model**

The microfabrication process involved in the manufacture of MEMS based accelerometers results in relatively well-behaved Wheatstone bridge sensing elements with controlled sensitivity and unstrained (zero G) bridge balance. However, an inherently large unit to unit variation exists in the bridge resistance properties of the final accelerometer assembly. This was clearly shown in TABLE 1 of this report where output resistance of various range sensors of the same model varied by *a factor of more than 2 to 1*. The test planner must be aware of this large resistance variation and its effect on the roll-off and desensitization characteristics of the cable/sensor pair. Swapping of sensors during test and/or field repair of damaged cables further complicate this process. Methodologies such as 6 wire remote excitation sense<sup>8</sup> and PFI's AC shunt cal<sup>9</sup> technique can be very helpful in managing these issues.

TABLE 7 (below) quantifies how the unit-to-unit variations in resistance impacts the maximum allowable cable length to comply with the default (10 KHz) frequency specified in MIL-STD 810H Annex A. TABLE 8 similarly quantifies how the unit-to-unit variations in accelerometer sensor input resistance impacts the accelerometer sensitivity at all frequencies.

Two examples will illustrate the application of TABLES 7 and 8. The examples will provide assessment across the *total range* of possible output resistances for each model. Recall, the goal is to achieve flat frequency response within +/- 1 dB to 10 KHz while managing any decrease in the accelerometer's sensitivity.

Variation in Max Cable Length for < -1dB Roll-Off @10kHz (ft)			
Cable Type	PCB 3501 (Max Rout/Min Rout)	Endevco 7270 (Max Rout/Min Rout)	Endevco 7280 (Max Rout/Min Rout)
Belden 82502	44/88	369/966	39/88
PCB 096	53/106	403/762	47/106
PCB 034	72/143	544/1042	64/143

**TABLE 7. Variation of max cable length for -1dB cable roll-off at 10 kHz for various cable/sensor pairs based on variations in Rout as shown in TABLE 1.**

Variation in sensor desensitization caused by sensor input resistance (%)									
Cable Type	Added Cable length = 50 ft			Added Cable length = 100 ft			Added Cable length = 150 ft		
	PCB 3501	Endevco 7270	Endevco 7280	PCB 3501	Endevco 7270	Endevco 7280	PCB 3501	Endevco 7270	Endevco 7280
Belden 82502	0/0.1	0.3/0.7	0/0.1	0.1/0.1	0.5/1.4	0.1/0.1	0.1/0.2	0.8/2.0	0.1/0.2
PCB 096	0.5/1.0	4.2/10.7	0.5/1.0	1.0/2.1	8.1/19.4	0.9/2.1	1.6/3.1	11.7/26.5	1.4/3.1
PCB 034	0.4/0.7	3.0/7.7	0.3/0.7	0.7/1.4	5.8/14.3	0.6/1.4	1.1/2.2	8.5/20.1	1.0/2.2

**TABLE 8. Range of errors possible due to additional spliced cable (assumes length of sensor's integral cable to be negligible).**

#### Examples Based on Default Requirement of 10 KHz:

**Example 1:** Consider an Endevco 7280A model accelerometer possessing the lowest specified output impedance for that model of 4000Ω. Assume that we are using Belden 82502 cable. Per TABLE 7, according to the methods and calculations presented in this paper, one can satisfy the default frequency requirements of the referenced MIL-STD with up to 88 feet of this cable. Assessing TABLE 8, the same accelerometer's sensitivity is decreased by less than 0.1% due to its high output resistance. Thus, for 88 ft of this Belden cable, compliance can be assured for this most optimal 4000Ω output impedance with the default 10 KHz requirement of the MIL-STD. However, the output impedance of the 7280A model can vary between 4000 and 9000 ohms. *If a random selection among 7280A's resulted in an output resistance of 9000 ohms, any cable length over 39 feet (per TABLE 7) would not satisfy the 10KHz requirement.*

**Example 2:** Consider whether the selection of an Endevco 7270A model accelerometer with the addition of 100 feet of spliced PCB 034 cable will satisfy the default 10kHz frequency requirement of the referenced MIL-STD. Per TABLE 7, it is clear that any randomly selected 7270A would easily meet this requirement with regard to pass-band flatness. *However, assessing TABLE 8, if sensor supply voltage is not corrected at the cable splice the desensitization created by the choice of 7270A's would create a uniform error at all frequencies of between 5.8 and 14.3 percent.*

## SUMMARY

The completion of this work required cooperation between a sensor developer/manufacture, a developer/manufacture of precision analog signal conditioning, and a supporting university over a one-year period. Although separated by significant distances and the travel and interaction protocols of COVID-19, the communications technology of today enabled a detailed research, test, and analysis activity to be carefully implemented. The result was additional knowledge and guidance that should be incorporated into the specification and standards for instrumentation systems intended to measure severe shock. This guidance is of particular importance as it impacts the qualification testing of aerospace and defense (A&D) systems expected to operate and function under conditions of severe shock. Accurately measured shock inputs to critical components in the full-scale development testing phase of A&D systems provide the basis for qualification of subsequent production builds of these components. In turn, properly qualified components ensure the reliability of any full-scale system over its projected storage and usage lifetime.

To acquire critical high-frequency shock information to support A&D system reliability, a measurement system must be designed to operate within its linear range while providing an overall frequency response function (amplitude and phase characteristics) compatible with established test objectives. The order sequence of the individual measurement system components is also important.

The initial component in the measurement system is the accelerometer, which contains the MEMS sensing element. The structural dynamics of the accelerometer housing, the method and quality of attachment of this housing to the unit under test (UUT), the interface of the MEMS element to the housing, and the mechanical interface of the cable to the MEMS element combine to define the initial frequency response function in the measurement system.<sup>5</sup> This response function is defined by the structural dynamics of the accelerometer assembly in its mounted configuration.

The next frequency response function in the measurement system, which was the subject of this work, is that associated with the accelerometer cable. The individuality of the cable is largely ignored for analysis as a separate component in the measurement chain. This work has proven that two accelerometers of the same model and range can have greatly differing frequency response functions attributable to differences in both the output resistance of their MEMS sensing elements and the distributed electrical impedances of their cables.

Measurement system standards for severe shock are typically specified around wideband differential amplifiers, data sampling rates of 1 MHz or higher, and sophisticated antialiasing filters. This work has definitively proven that oftentimes the high frequency information that these systems are designed to accommodate never exits the accelerometer cable. Methods both to analytically and experimentally characterize cables in the laboratory, as well as hardware to enable characterization in the field, have been described.<sup>6</sup> *The cable is the too often ignored, but critically important, component in the measurement system.*<sup>4,6</sup>

**Acknowledgement:** The predictive modeling of the sensor/cable frequency response combination in this report was performed within Precision Filters, Inc. and coordinated by Alan Szary, V.P engineering. *For derivation and verification of the predictive equations, the reader is strongly encouraged to acquire Reference 6.* James Woernley, PFI engineer, was tireless in acquiring shock data to illustrate the necessity to characterize the measurement system pretest to assure meaningful test data is acquired. Bob Metz,

Director of Aerospace and Development at PCB, supported this activity throughout with funding and hardware. I express my gratitude to all of them.

*I personally dedicate this work to James Lally (deceased), co-founder (with his brother Robert) and CEO emeritus of PCB, and Prof. Peter K Stein (deceased), Arizona State University, both former Lifetime Achievement Award winners in S&V, who dedicated their careers to advancing measurement science.*

Patrick L. Walter  
Sandia National Labs (retired)  
TCU Engineering Dept. (retired)

## References:

1. Agnello, Anthony; Dosch, Jeff; Metz, Robert; Sill, Robert; and Walter, Patrick; *Acceleration Sensing Technologies for Severe Mechanical Shock*, PCB Piezotronics, Inc. White Paper #45
  - also published in: *Sound and Vibration*, pp. 8-19, February 2014.
2. Agnello, Anthony; Smith, Strether; Sill, Robert; and Walter, Patrick; *Evaluation of Accelerometers for Pyroshock Performance in a Harsh Field Environment*, PCB Piezotronics, Inc. White Paper #60.
3. Walter, Patrick L., *Acquiring Meaningful Test Data on Purpose*, *Sound and Vibration*, editorial, pp.2-3, March 2016.
4. Walter, Patrick L., *The Instrumentation Cable: Critical but Often Neglected*, PCB Piezotronics, Inc. Tech Note-33 (TN-33), 2015.
5. Walter, Patrick L., *How High in Frequency are Accelerometer Measurements Meaningful*, PCB Piezotronics, Inc. Tech Note-25 (TN-25), 2009.
6. Szary, Alan, et al., *Methods and Procedures for Predicting Cable Roll-off in Sensor Measurements, Part I: Full Bridge measurements*, Precision Filters. Inc. White Paper, 2020.
7. Lamb, H.A., *On the Oscillations of a Viscous Spheroid*, London Mathematical Society, pp. 51-70, Nov. 1, 1881.
8. Perino, Peter R., *System Considerations for Bridge Circuit Transducers*, Statham Instrumentation Notes, 1964.
9. Precision Filters Inc. LP8FP Specification sheet, (P8477 Rev C)
10. AC shunt Cal technique described in 28124 Specification sheet (P8465 Rev F), Pg. 4, Precision Filters Inc.

# APPENDIX A.1

## MEMS Test Accelerometer Calibration Certificates

### ~ Calibration Certificate ~

**Model Number:** 3591B1220KG  
**Serial Number:** 11009  
**Manufacturer:** PCB  
**Description:** Piezoresistive Accelerometer  
**Method:** ISO 16063-22

**Test Data**

<b>Sensitivity @ Ref. Level:</b> 9.148 $\mu\text{V/g}$ (0.933 $\mu\text{V}/\text{m/s}^2$ )	<b>Excitation Voltage:</b> 10.00 Volts
<b>Reference Input Level:</b> 5000 g (49033.2 $\text{m/s}^2$ )	<b>Offset Voltage:</b> 1.0 mV
<b>Pulse Duration:</b> 0.25 msec	<b>Input Resistance:</b> 6241 Ohms
<b>Temperature:</b> 73°F (23°C)	<b>Output Resistance:</b> 6543 Ohms
	<b>Humidity:</b> 42 % RH

**Condition of Unit**

As Found: n/a  
As Left: New Unit, In Tolerance

**Notes**

- This calibration is the result of averaging 3 shock pulses at the reference level. Calibration traceable to primary method which has been proficiency validated interlaboratory comparison to NIST project number 822271196.
- This certificate shall not be reproduced, except in full, without written approval from PCB Piezotronics, Inc.
- Calibration is performed in compliance with ISO 9001, ISO 10012-1, ANSI/INCISL Z340-1-1994, and ISO 17025.
- See Manufacturer's Specification Sheet for a detailed listing of performance specifications.
- Measurement uncertainty (95% confidence level with coverage factor of 2) for amplitudes 20 to 2,000 g's pk;  $\pm 1.9\%$  and for amplitudes > 2k to 10k g's;  $\pm 2.6\%$ .

**Technician:** John Pattison (JP 1174)      **Cal Date:** 4/20/2020  
**Station:** CAL139

3425 Walden Avenue • Dayton, New York 14043  
 Tel: 888-684-0013 • Fax: 716-893-3886 • www.pcb.com

Cal ID: CAL139-362035959

### Calibration Certificate

**Document number:** 160688  
**Description:** 4 Arm PR accelerometer  
**Manufacturer:** ENDEVCO  
**Model Number:** 7270A-20KIM4  
**Serial Number:** 11693

**Sensitivity:** 6.732  $\mu\text{V/g}$   
 0.8904  $\mu\text{V}/\text{m/s}^2$

**Pulse Duration:** 0.123 ms  
**Shock Level:** 5130 g  
 50305  $\text{m/s}^2$

**Excitation:** 10.0 V

**Temperature (°C):** 22    (°F): 71  
**Relative Humidity (%):** 41  
**Input Resistance (ohms):** 570  
**Output Resistance (ohms):** 577  
**ZMO (mV):** 26.8

**Notes:**

**Figure number:** \_\_\_\_\_  
**Uncertainty estimate (95% confidence, k=2)**  
 +/- 1.7 %    100.0 < a <= 2000.0 g  
 +/- 2.5 %    2000.0 < a <= 10000.0 g

**Traceability:**  
 Ref Manufacturer: ENDEVCO  
 Ref Model number: 2270  
 Ref Serial number: 14117  
 Traceability #: NIST 683/290325-18

**Equipment and procedures used:**  
 Console S/N: AC35  
 Exciter name: POP  
 Test Name: FINAL POP REV E

**By:** \_\_\_\_\_  
 CANDO, VICTORIA  
 Test Date: 4/17/2020    6:25 AM  
 Print Date: 4/17/2020  
 MDC - HRM  
 s/w 11.7

**ACCREDITED**  
 CALIBRATION CERT #1882.02

ED455 Rev R  
 Page 1 of 1

This instrument was tested using comparison calibration on Endevco's Automated Accelerometer Calibration System (AACS) PN 6837. This calibration is traceable to the National Metrology Institute (NMI: NIST, PTB, etc.) and is in accordance with ISO/IEC 17025:2005 and ANSI/INCISL Z340-1-1994 (MIL-STD-4883A). Test procedure follows CL-TP-004, Transverse Sensitivity, when provided, was calibrated with uncertainty at 0.27% of output. This certificate shall not be reproduced, except in full, without written approval of PCB Piezotronics of NC, Inc. ©2016 Endevco.

~ Calibration Certificate ~

Model Number: 7280A314-20K  
 Serial Number: 11417  
 Manufacturer: ENDEVCO  
 Description: Piezoresistive Accelerometer  
 Method: ISO 10603-22

**Test Data**

Sensitivity @ Ref. Level: 21.080 $\mu\text{V/g}$ (2.150 $\mu\text{V/ms}^2$ )	Excitation Voltage: 10.04 Volts
Reference Input Level: 5000 g (4903.2 $\text{ms}^{-2}$ )	Offset Voltage: 5.7 mV
Pulse Duration: 0.21 msec	Input Resistance: 4662 Ohms
Temperature: 73°F (23°C)	Output Resistance: 4668 Ohms
	Humidity: 50 % RH

Reference  SUT

**Condition of Unit**

As Found: In Tolerance  
 As Left: In Tolerance

**Notes**

1. This calibration is the result of averaging 3 shock pulses at the reference level. Calibration is N.I.S.T. Traceable through Project 6843-0000008831.
2. This certificate shall not be reproduced, except in full, without written approval from PCB Piezotronics, Inc.
3. Calibration is performed in compliance with ISO 10012-1, ANSI/INCIL Z540.3 and ISO 17025.
4. See Manufacturer's Specification Sheet for a detailed listing of performance specifications.
5. Measurement uncertainty (95% confidence level with coverage factor of 2) for amplitudes 20 to 2,000 g's pk:  $\pm 1.9\%$  and for amplitudes > 2k to 10kg pk:  $\pm 2.6\%$

Technician: Jeffrey Mattison Cal Date: 11/11/2020

Station: CAL79

Page 1 of 1

3625 HAZELTON DRIVE • TORONTO, ON CANADA  
 TEL: 888-684-6013 • FAX: 718-681-3886 • www.pcb.com

Cal ID: CAL79-348791-1923-0

## APPENDIX A.2

### Mechanically-Isolated & Electrically-Filtered ICP® Reference Accelerometer Calibration Certificates

**~ Calibration Certificate ~**  
Per ISO 16063-21

Model Number: 350D02  
Serial Number: 55372  
Description: ICP® Shock Sensor  
Manufacturer: PCB Method: Back-to-Back Comparison AT401-3

**Calibration Data**

Sensitivity @ 100 Hz    0.104 mV/g    Output Bias    10.2 VDC  
(0.0106 mV/m/s²)    Transverse Sensitivity    3.0 %

**Sensitivity Plot**

Temperature: 70 °F (21 °C)    Relative Humidity: 72 %

Data Points			
Frequency (Hz)	Dev. (%)	Frequency (Hz)	Dev. (%)
REF. FREQ.	0.0	5000	-0.3
300	-0.1	7000	-0.5
500	-0.3	10000	-0.8
1000	-0.2		
3000	-0.2		

Mounting Surface: See Data Sheet - Reference Center    Fixtures: 1A-28 N/A    Fixtures Orientation: Vertical  
Amplification Level: 100 (10.0 dB)    100.0 (20.0 dB)  
\*The acceleration level may be limited by fixture displacement at low frequencies. If the fixed level cannot be obtained, the calibration system uses the following formula to set the vibration amplitude: Acceleration Level (g) = 0.008 x (Level) \* The gain factor is used for calculations by the calibration system. (g = 9.80665 m/s²)

**Condition of Unit**

As Found: In Tolerance  
As Left: In Tolerance

**Notes**

1. Calibration is NIST Traceable thru Project 683/287323 and PTB Traceable thru Project 17014.
2. This certificate shall not be reproduced, except in full, without written approval from PCB Piezotronics, Inc.
3. Calibration is performed in compliance with ISO 9001, ISO 10012-1, ANSI Z540.3 and ISO 17025.
4. See Manufacturer's Specification Sheet for a detailed listing of performance specifications.
5. Measurement uncertainty (95% confidence level with coverage factor of 2) for frequency ranges tested during calibration are as follows: 5-9 Hz: +/- 2.0%, 10-99 Hz: +/- 1.5%, 100-1999 Hz: +/- 1.0%, 2-10 kHz: +/- 2.5%.

Technician: Ronald Stevens    Date: 6/23/2017

**PCB PIEZOTRONICS™**  
VIBRATION DIVISION  
3425 WALDEN AVENUE - DEPEW, NY 14043  
TEL: 888-684-0013    FAX: 716-685-3888    www.pcb.com

**~ Calibration Certificate ~**  
Per ISO 16063-21

Model Number: 350D02  
Serial Number: 66366  
Description: ICP® Shock Sensor  
Manufacturer: PCB Method: Back-to-Back Comparison AT401-3

**Calibration Data**

Sensitivity @ 100 Hz    0.104 mV/g    Output Bias    11.5 VDC  
(0.0106 mV/m/s²)    Transverse Sensitivity    1.9 %

**Sensitivity Plot**

Temperature: 72 °F (22 °C)    Relative Humidity: 31 %

Data Points			
Frequency (Hz)	Dev. (%)	Frequency (Hz)	Dev. (%)
REF. FREQ.	0.0	5000	0.3
300	-0.1	7000	-0.4
500	-0.0	10000	-0.1
1000	0.3		
3000	0.1		

Mounting Surface: See Data Sheet - Reference Center    Fixtures: 1A-28 N/A    Fixtures Orientation: Vertical  
Amplification Level: 100 (10.0 dB)    100.0 (20.0 dB)  
\*The acceleration level may be limited by fixture displacement at low frequencies. If the fixed level cannot be obtained, the calibration system uses the following formula to set the vibration amplitude: Acceleration Level (g) = 0.008 x (Level) \* The gain factor is used for calculations by the calibration system. (g = 9.80665 m/s²)

**Condition of Unit**

As Found: n/a  
As Left: New Unit, In Tolerance

**Notes**

1. Calibration is NIST Traceable thru Project 683/287323 and PTB Traceable thru Project 17014.
2. This certificate shall not be reproduced, except in full, without written approval from PCB Piezotronics, Inc.
3. Calibration is performed in compliance with ISO 10012-1, ANSI Z540.3 and ISO 17025.
4. See Manufacturer's Specification Sheet for a detailed listing of performance specifications.
5. Measurement uncertainty (95% confidence level with coverage factor of 2) for frequency ranges tested during calibration are as follows: 5-9 Hz: +/- 2.0%, 10-99 Hz: +/- 1.5%, 100-1999 Hz: +/- 1.0%, 2-10 kHz: +/- 2.5%, 10-15 kHz: +/- 5%.

Technician: Mary Warren    Date: 3/23/2020

**PCB PIEZOTRONICS™**  
VIBRATION DIVISION  
3425 WALDEN AVENUE - DEPEW, NY 14043  
TEL: 888-684-0013    FAX: 716-685-3888    www.pcb.com

**APPENDIX B**

**PFI LP8FP Filter Specification**

# LP8F & LP8P

## 8-POLE, 8-ZERO FLAT/PULSE LOW-PASS FILTER



### DESCRIPTION

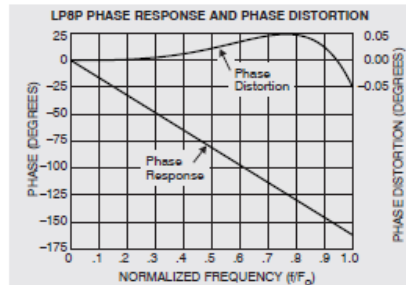
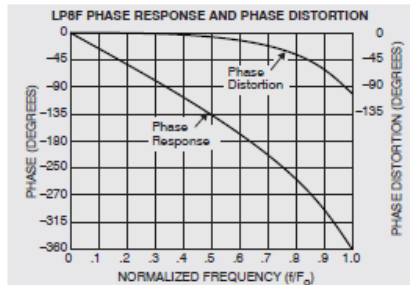
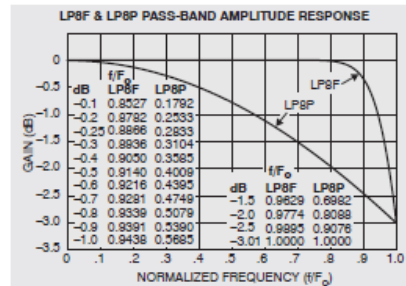
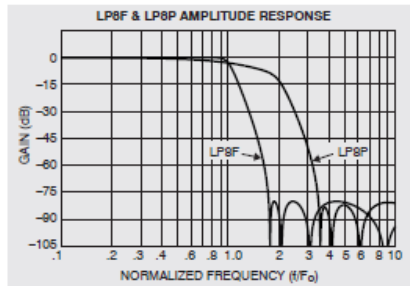
The LP8F and LP8P 8-pole, 8-zero Low-Pass filters together provide the user with the versatility to address applications in either the time or frequency domain. The choice of LP8F or LP8P is programmable in most Precision Filters products that offer this filter characteristic.

The LP8F is specified to have outstanding pass-band flatness and very sharp roll-off characteristics. The pass-band characteristic is nearly identical to an 8-pole Butterworth yet the LP8F has a much sharper roll-off. The LP8F is a good choice as an anti-aliasing filter and for applications such as spectral analysis. The LP8P has excellent transient response and phase linearity making it an ideal filter for time domain applications including transient (shock) measurements and time domain waveform analysis. The LP8P has frequency domain characteristics superior to the 8-pole Bessel filter. Like the Bessel, the LP8P has a broadly rounded amplitude response that is a consequence of the LP8P's linear phase property.

Cascade an HP8F with an LP8F to form a band-pass filter. If the filters are set with the  $-0.1$  dB frequencies overlapping, the resulting band-pass filter will have 0.2 dB of insertion loss and will provide more than 80 dB of attenuation below  $0.487 F_c$  and above  $2.05 F_c$ .

### SPECIFICATIONS

	LP8F Maximally Flat Low- Pass Filter	LP8P Constant Time Delay Low-Pass Filter
Cutoff Frequency Amplitude	-3.01 dB	-3.01 dB
DC Gain	0.00 dB	0.00 dB
Pass-Band Ripple	0.00 dB	0.00 dB
Stop-Band Frequency:	1.7479 $F_c$	3.4688 $F_c$
Cutoff Frequency Phase	-360.0°	-161.9°
Phase Distortion (DC to $F_c$ )	<102.0°	<0.05°
Zero Frequency Group Delay	0.7197/ $F_c$	0.4496/ $F_c$
Percent Overshoot	18.9%	1.1%
1% Settling Time	4.03/ $F_c$	1.25/ $F_c$
0.1 % Settling Time	7.02/ $F_c$	2.25/ $F_c$
-0.1 dB Frequency	0.8527 $F_c$	0.1792 $F_c$
-1 dB Frequency	0.9438 $F_c$	0.5685 $F_c$
-2 dB Frequency	0.9774 $F_c$	0.8088 $F_c$
-3.01 dB Frequency	1.0000 $F_c$	1.0000 $F_c$
-20 dB Frequency	1.2152 $F_c$	2.2342 $F_c$
-40 dB Frequency	1.4443 $F_c$	2.7556 $F_c$
-60 dB Frequency	1.6391 $F_c$	3.2016 $F_c$
-80 dB Frequency	1.7479 $F_c$	3.4688 $F_c$





**3425 Walden Avenue, Depew, NY 14043 USA**

pcb.com | info@pcb.com | 800 828 8840 | +1 716 684 0001

© 2022 PCB Piezotronics - all rights reserved. PCB Piezotronics is a wholly-owned subsidiary of Amphenol Corporation. Endevo is an assumed name of PCB Piezotronics of North Carolina, Inc., which is a wholly-owned subsidiary of PCB Piezotronics, Inc. Accumetrics, Inc. and The Modal Shop, Inc. are wholly-owned subsidiaries of PCB Piezotronics, Inc. IMI Sensors and Larson Davis are Divisions of PCB Piezotronics, Inc. Except for any third party marks for which attribution is provided herein, the company names and product names used in this document may be the registered trademarks or unregistered trademarks of PCB Piezotronics, Inc., PCB Piezotronics of North Carolina, Inc. (d/b/a Endevo), The Modal Shop, Inc. or Accumetrics, Inc. Detailed trademark ownership information is available at [www.pcb.com/trademarkownership](http://www.pcb.com/trademarkownership).

WPL\_85\_0222